タイトル Title	Acidic Property of BEA Zeolite Synthesized by Seed-directed Method
著者 Auther(s)	Suganuma, Satoshi; Zhang, Haiyan; Yang, Chengguang; Xiao, Feng-Shou; Katada, Naonobu
掲載誌・巻号・ページ Citation	Journal of porous materials , 23 (2) : 415 - 421
刊行日 Issue Date	2016
資源タイプ Resource Type	学術雑誌論文 / Journal Article
版区分 Resource Version	著者版 / Author
権利 Rights	© Springer Science+Business Media New York 2015
DOI	10.1007/s10934-015-0095-6
URL	http://repository.lib.tottori-u.ac.jp/5726

Acidic Property of BEA Zeolite Synthesized by Seed-directed Method

Satoshi Suganuma*[1], Haiyan Zhang[2], Chengguang Yang[2], Feng-Shou Xiao[3], and Naonobu Katada[4]

1 Center for Research on Green Sustainable Chemistry, Graduate School of Engineering, Tottori University, 4-101 Koyama-cho Minami, Tottori 680-8552, Japan

2 State Key Lab of Inorganic Synthesis and Preparative Chemistry, Jilin University, Changchun 130012, China

3 Key Lab of Applied Chemistry of Zhejiang Province, Zhejiang University, Hangzhou 310028, China

4 Department of Chemistry and Biotechnology, Graduate School of Engineering, Tottori University, 4-101 Koyama-cho Minami, Tottori 680-8552, Japan

* Corresponding author, suganuma@chem.tottori-u.ac.jp Phone/fax +81-857-31-5684

Abstract

The acidic property of a BEA zeolite prepared by a seed-directed synthesis (SDS) method without organic structure directing agent (OSDA) was analyzed by a method of ammonia infrared / mass spectroscopic (IRMS) temperature-programmed desorption (TPD). The number of Brønsted acid sites on the SDS-BEA zeolite was larger than that on a conventional BEA zeolite synthesized from using OSDA. The enthalpy of ammonia desorption, distributed mainly in a range between 115 and 145 kJ mol^{-1}, was in agreement with the acid strength region generated by isomorphous substitution of Si^{4+} by Al^{3+} in the BEA framework. These observations confirm that the microstructure around the incorporated Al in the SDS-BEA zeolite was equivalent to that in the conventional one.

Keywords

BEA zeolite; Acidic property; Seed-directed synthesis; OSDA-free

Introduction

Zeolite with a *BEA structure (zeolite β, hereafter BEA zeolite) shows high catalytic activities generally for alkylation [1] and acylation reactions including so-called Friedel-Crafts type reactions in liquid phase [2]. Therefore this type of zeolite is promising for use in chemical industries in place of liquid acid catalysts, as strongly demanded from a view of environmental protection [3]. Its characteristic microporous structure consisting of 12-ring (12 oxygen-membered ring) channels is believed to show the efficient activities for reactions of relatively large molecules, as supported by a theoretical study [4]. In addition, the strong or moderate Brønsted acid sites, generated by isomorphous substitution of Si^{4+} by Al^{3+}, are the origin of catalytic activity.

Niwa et al. have developed a method of ammonia infrared / mass spectroscopic (IRMS) temperature-programmed desorption (TPD) [5], and have measured the Brønsted acid strength of the BEA zeolite prepared by a dry gel conversion (DGC) method [6]. The enthalpy of ammonia desorption (hereafter ΔH) was within 120 - 140 kJ mol^{-1} [7, 8]. The values of ΔH on industrially important zeolites were shown to be MOR > MWW > MFI > BEA > FAU [9]. The sequence MFI > BEA > FAU in acid strength was generally in agreement with such preceding studies as those based on microcalorimetry of ammonia [10], infrared (IR) spectroscopy of adsorbed N_2 [11] and hydrocarbon reactivity [12,13]. It means that the stronger Brønsted acid sites can be found in the MWW and MFI zeolites, but in the crystals of these zeolites, reactant molecules must pass 10-rings to reach most of the active sites: the MWW zeolite has 12-ring-sized cavities, but they are connected by 10-ring channels, and therefore without specific techniques to create mesopores, to delaminate [14] or to enlarge interlayer spaces [15], the molecules have to pass 10-rings to reach the 12-ring cavity. The MOR zeolite may have both of 12-ring channels and strong Brønsted acid sites (its intrinsic strength is a subject of discussion [16]), but strong acid sites are mainly located in 8-ring

channels [5]. The FAU zeolite has a supercage connected by 12-ring channels, but its original Brønsted acid site is weak (ΔH = 100-110 kJ mol^{-1}) [17], unless specific modification with extraframework cation species is carried out [18]. Thus, the BEA type is only the species possessing the Brønsted acid sites due to the isomorphous substitution of Si^{4+} by Al^{3+} with moderate acid strength in the 12-rings among aluminosilicate zeolites applied as catalysts to industrial processes.

More than half of the cost for industrial production of zeolite is owing to the use of organic structure directing agent (OSDA) especially in cases where the composition of zeolite is highly siliceous. Therefore, OSDA-free synthesis methods have been studied extensively. Xie et al. have recently developed a method of OSDA-free synthesis of the BEA zeolite using seed crystals [19,20]. Other research groups also presented the synthesis of BEA by seeding [21,22]. Crystalline and textual properties of the BEA zeolite prepared by the seed-directed synthesis method (hereafter, SDS-BEA) have been analyzed to show the high crystallinity comparable to the conventional sample synthesized in the presence of OSDA. A high catalytic activity for cracking of light vacuum gas oil has been found [20].

From a view of catalytic application, the acidic property, especially the number and strength of Brønsted acid sites, should be the subject of discussion. Particularly, the comparison of acidic properties between the SDS sample and conventional BEA should be necessary to establish a truly practical method. The ammonia IRMS-TPD method has been applied to the BEA zeolite to find the acid strength sequence MFI > BEA > FAU as above [7]. We apply the same method to these BEA zeolites in the present study in order to evaluate the acid properties of BEA zeolites.

Methods

1. Experimental

The synthesis of SDS-BEA zeolite without OSDA was carried out as follows. As reported

[19], 0.07 g of $NaAlO_2$ and 0.312 g of NaOH were dissolved in 8.64 cm^3 of H_2O, followed by addition of 0.72 g of fumed silica. After stirring for 10 min, 0.086 g of Beta zeolite seeds were introduced into the gel. After a further stirring for 3 min, the mixture was transferred into an autoclave to crystallize at 413 K for 18.5 h. Products were obtained by filtration at room temperature and drying at about 353 K. The elemental analysis showed that the Si/Al molar ratio was 5.3, as already reported [19].

In comparison, a sample of BEA zeolite with Si/Al = 5.3 was prepared in the presence of OSDA (hereafter, cntl -BEA). At first, 0.16 g of NaOH and 0.30 g of $NaAlO_2$ were dissolved in 30 cm^3 of tetraethylammonium hydroxide (TEAOH, 20 wt%), then 4.8 g of fumed silica was added. After stirring for 1 h at room temperature, the mixture was transferred into an autoclave to crystallize at 413 K for 120 h. The product was collected by centrifugation, dried in air, and calcined at 823 K for 5 h to remove the OSDA. In addition, a sample with Si/Al = 12.5 was supplied by Catalysis Society of Japan as a reference catalyst JRC-Z-B25 (1). This catalyst is Na-form zeolite similar to SDS-BEA and cntl-BEA.

The H-form of BEA zeolites were obtained by ion-exchange with 1 mol dm^{-3} NH_4NO_3 solution at 353 K for 3 h (1 g of zeolite in 50 cm^3 of solution), followed by calcination at 773 K for 3 h. This ion-exchange process was repeated twice. The H-form samples were prepared from SDS- and cntl-BEA, and JRC-Z-B25.

The Ammonia IRMS-TPD method was carried out using an automatic IRMS-TPD analyzer (MicrotracBEL). The measurement conditions referred to our previous paper, in which homemade IRMS-TPD analyzer was used [5]. The powder samples (5.5, 6.8, and 3.9 mg of SDS- and cntl -BEA, and JRC-Z-B25, respectively) were compressed into a self-supporting disk with 1 cm of the diameter under ca. 20 MPa of the pressure. The disk was placed in an in-situ IR cell equipped with an electric furnace. The cell was evacuated, 100 kPa of oxygen was introduced in flow of 37 μmol s^{-1}, and then heated at a ramp rate of 10 K min^{-1} up to 823 K. After 1 h of the pretreatment in oxygen at 823 K, the

cell was evacuated at 823 K for 20 min. IR spectra were recorded before and after NH_3 adsorption. A helium flow (89 μmol s^{-1}) was introduced to pass through the IR cell. The sample was heated at a ramp rate of 2 K min^{-1} during the elevation temperature from 373 to 803 K in a helium flow at 6.0 kPa, and an IR spectrum was collected before ammonia adsorption at an interval of 0.5 min. These IR spectra will be referred as background spectra $N(T)$ hereafter. The temperature was subsequently cooled down to 343 K, supply of the helium flow was stopped, the cell was evacuated, and ammonia (13 kPa) was kept contact with the sample disk at 343 K for 30 min. The gaseous ammonia was then removed by evacuation at 343 K for 30 min, and the helium flow was again. After the stabilization step, the temperature was elevated. The flow rate of helium (89 μmol s^{-1}), total pressure (6.0 kPa) and ramp rate (2 K min^{-1}) were the kept as those employed before the ammonia adsorption. IR spectrum [sample spectrum $A(T)$] was taken at each 1 K, and a mass spectrum at m/e = 16 showing NH_3 was collected using a mass spectrometer (MS) during the temperature elevation. Other selected signals of mass spectrum with different m/e ratios were also recorded in order to confirm that the signal at m/e = 16 did not contain noises due to other materials such as water and carbon dioxide. Finally an ammonia/helium mixture with a known concentration of ammonia (1 - 4 $\times 10^{-5}$ mol m^{-3}) was fed to the mass spectrometer to calibrate the intensity.

Results

IR spectra of the BEA zeolites after pretreatment at 373 K is shown in Figure 1. Two signals for stretching mode of Si-OH (ca. 3745 cm^{-1}) and acidic OH (ca. 3610 cm^{-1}) were observed in each spectrum. The peak at 3660 cm^{-1} assignable to acidic OH was detected in the spectrum of SDS-BEA (Figure 1 (A)).

Figure 2 shows IR spectra [difference spectra $A(T)$-$N(T)$] displaying the influence of

ammonia adsorption on zeolite. The thermal behaviors of -OH stretching vibration on the catalysts are shown in Figure 3. The negative absorption peaks at 3743-3722 and 3607-3582 cm^{-1} ascribed to the terminal Si-OH and the framework bridged OH groups was observed in these spectra [23,24]. In the spectra of SDS- and cntl-BEA (Figure 3 (A), (B)), the detected negative absorption peak at 3783-3756 cm^{-1} was assignable to terminal Al-OH [23,24]. The negative absorption peak at 3654-3643 cm^{-1} was found in the spectrum of SDS-BEA, at the similar peak position in Figure 1 (A). It is speculated that this peak corresponds to Al-OH where the aluminum atom is connected with the zeolite framework only by one or two remaining chemical bonds [24]. These results indicate that SDS-BEA possesses four types of OH groups than the other BEA zeolites. The thermal behaviors of ammonia desorption from Brønsted and Lewis acid sites were analyzed from bending vibrations shown in Figure 4. At a low temperature, a band of NH_4 species presumably NH_4^+ cations bonded to Brønsted acid sites was observed at 1450 cm^{-1}; the vibration mode is shown in Figure 5 (A) [25]. A band due to NH_3 coordinated to the Lewis acid sites around 1320 cm^{-1} [26] was small. The intensities of these bands were quantitatively evaluated by deconvolution of the spectrum as shown in Figure 6. Differentiation of the peak intensities by the temperature gives IR-TPD spectra, i.e., the relative desorption rates of ammonia, from Brønsted and Lewis acid sites as functions of the temperature. Quantification of the Brønsted and Lewis acid sites was carried out by fitting the MS-TPD and sum of IR-TPDs of Brønsted and Lewis acid sites multiplied with adjusted coefficients, as shown in Figure 7, based on the assumption that the sum of numbers of ammonia molecules desorbed from Brønsted and Lewis acid sites were equal to the number of ammonia detected by MS. By this procedure, the TPD spectrum of Brønsted and Lewis acid sites are obtained with the vertical axis in the unit of mol m^{-3}.

On the cntl-BEA and JRC-Z-B25, a separated peak at ca. 400 K in the MS-TPD was not observed in the IR-TPDs of Brønsted and Lewis acid sites. The 400 K-peak of ammonia TPD, so-

called *l*-peak (low temperature peak) is ascribed to NH_3 hydrogen-bonded to NH_4 which had been formed on the Brønsted acid site [27-29]. It has been known that the wavenumber of NH_3-M strongly depends on the element of M [26], and therefore the hydrogen-bonded NH_3 must have the band position and width different from those of Lewis acid site-bounded NH_3, and it is possible that the former is hidden by the skeletal absorption of zeolite. In conclusion, we can say that there was at least one kind of NH_3 species bonded to non-acidic adsorption site, and it was ignored by the IRMS analysis. Also on the SDS-BEA, the low temperature part of MS-TPD was not fitted with the IR-TPDs and therefore ignored.

Figure 7 shows the MS-TPD spectra whose vertical axis is shown in the unit of mol m^{-3}. The integration of desorption peak gives the total number of ammonia molecules adsorbed, which should be equal to the number of acid sites (hereafter A_0), as listed in Table 1. The Lewis acid sites were less than the Brønsted acid sites. The strength distribution of Brønsted acid sites was analyzed according to a method previously proposed [30]. The desorption profile is calculated based on assumed distribution of ammonia adsorption heat, and the distribution which gave the curve fitted best to the experimental curve (Figure 8) was selected as shown in Figure 9.

Discussion

Number (A_0) and strength (ΔH) of the Brønsted and Lewis acid sites on the two samples were quantified in detail. Most of the acid sites were Brønsted type on both samples. The conventional BEA synthesized with using OSDA (cntl-BEA) had much smaller acid sites or much smaller Brønsted acid sites than the seed synthesized, SDA-free BEA (SDS-BEA). The numbers of Brønsted acid sites on the cntl-BEA and SDS-BEA was 14 and 25 % of the number of Al atoms (2.65 mol kg^{-1}), respectively. Cntl-BEA possesses octahedrally coordinated aluminum species [31] and

terminal Al-OH. Al atoms in SDS-BEA may exist as terminal Al-OH and AlO_4 tetrahedra partially connected with the zeolite framework [31]. The stoichiometric generation of acid sites where the number of Brønsted acid sites is equal or slightly smaller than the number of Al atoms is easily realized on the MOR and MFI structure,[32] but it is difficult to obtain on the BEA zeolite, probably due to the easiness of formation of crystallographic faults [33,34]. It has been shown that commercially available samples generally possessed the Brønsted acid sites less than 70% of Al content [7,35]. We have presented that the DGC method could realize the sample with Si/Al = 15 ([Al] = 1.0 mol kg^{-1}) in which the number of total acid sites were close to the number of Al atoms, but it had considerable fraction (16%) of Lewis acid sites [36], and it was impossible to obtain a sample with such a high quality at a lower Si/Al ratio, i.e., higher Al concentration [7]. In addition, the DGC method, to the best of our knowledge, has to use OSDA. We believe that the present Brønsted acid amount, 0.67 mol kg^{-1} and 25% of Al concentration, are sufficiently high to demonstrate the efficiency of OSDA-free synthesis method.

We have presented that the strength (or at least the ammonia desorption enthalpy ΔH from a view to avoid from a philosophical controversy about which parameter represents the intrinsic acid strength) of a Brønsted acid site generated by a framework Al atom is principally controlled by the framework structure and therefore the acid strength is small in one zeolite [9], and this is because the acid strength is controlled by the compression from the both ends of Al-OH-Si bridge induced by the forcefield due to the framework tension [37]. The peak position of ΔH distribution of Brønsted acid strength on cntl-BEA and JRC-Z-B25 was about 143 kJ mol^{-1}. However, the acid strength distribution of cntl-BEA was narrower than those of SDS-BEA and JRC-Z-B25. The distribution of ΔH on SDS-BEA was obviously broad compared to cntl-BEA and JRC-Z-B25, but ΔH of most of the Brønsted acid sites was within 115 - 145 kJ mol^{-1}. These are approximately consistent with previously reported values of ΔH on BEA, was in agreement with previous papers by us [7,9,13,36] and Collington et al.

[38,39] in which ΔH of the *BEA zeolite was ca. 130 kJ mol^{-1}, while the standard deviation was close to 10 kJ mol^{-1} [40]. In addition, density functional theory (DFT) calculations, which giving the ΔU (inner energy change) values generally consistent with the experimentally observed values over a wide range of zeolites, showed that acid sites at several crystallographically non-equivalent positions in the BEA structure possessed 127-133 kJ mol^{-1} of ΔU [8], corresponding to 132-138 kJ mol^{-1} of ΔH (= $\Delta U+RT_m$ where R and T_m are the gas constant and peak temperature of TPD, respectively) in the present experimental conditions. The presently observed range 115 - 145 kJ mol^{-1} was wider but different from the theoretically shown range 132 - 138 kJ mol^{-1}.

The ΔH distribution of the SDS-BEA was broader on low range. It had Brønsted acid sites exceptionally weak with ca. 120 kJ mol^{-1} of ΔH. On the other hand, the acid strengths of various zeolites are distributed from 100 to 160 kJ mol^{-1} [9]. From this knowledge, it has to say that the SDS-BEA contained a considerable amount of Al atoms whose structural environment was different from the Al atoms in proper *BEA zeolite. There are two possibilities.

[A] For example, some Al atoms in the SDS-BEA exist at the terminal on structural defects. Acidic OH around such irregular environments is speculated to be lower acid strength sites.

[B] Al was mainly contained in an amorphous region.

The latter has a low probability because the number of Lewis acid sites was small although the amorphous silica-alumina must have a large amount of Lewis acid sites, inconsistent with the fact that the SDS-BEA had negligible amount of Lewis acid sites. In the thermal behaviors of -OH stretching vibration on the catalysts (Figure 3), it is expected that SDS-BEA possesses defect sites, that brought formation of terminal Al-OH and OH group on AlO_4 tetrahedra partially connected with the zeolite framework. According to the DFT calculations [8], weaker acid sites were supposed to exist not at intersection of two 12-ring channels, but in a 12-ring channel. The generation of the defect sites in SDS-BEA may influence formation of the weaker acid sites in a 12-ring channel.

Therefore, OSDA-free method in the synthesis of SDS-BEA probably forms the weaker Brønsted acid sites, whereas it is difficult to form such weaker acid sites into the conventional BEA zeolites synthesized from using OSDA. It is concluded that most of Al atoms in the SDS-BEA generated Brønsted acidity equivalent to the conventional BEA zeolite, and a fraction of Al were in different environment to show slightly low Brønsted acid strength.

Conclusions

The BEA zeolite synthesized using no OSDA possessed little of Lewis acid sites. The number of Brønsted acid sites was ca. 25% of the number of Al atoms. Much of Al atoms may exist as terminal Al-OH and AlO_4 tetrahedra partially connected with the zeolite framework. The enthalpy of ammonia desorption of Brønsted acid sites as a measure of acid strength was 115-145 kJ mol^{-1}, approximately equivalent to the conventional zeolite with the same framework structure with a fraction of Brønsted acid sites with slightly low strength.

Acknowledgement

This study was partly supported by a Grant-in-Aid for Scientific Research (B) 23360358 from the Ministry of Education, Culture, Sports, Science and Technology, Japan.

[1] G. Bellussi, G. Pazzuconi, C. Perego, G. Girotti, G. Terzoni, J. Catal. 157 (1995) 227–234.

[2] G. Sartori, R. Maggi, Chem. Rev. 106 (2006) 1077–1104.

[3] K. Shimizu, A. Satsuma, Energy Env. Sci. 4 (2011) 3140–3153.

[4] C. Perego, S. Amarilli, R. Villini, G. Bellusi, G. Girotti, G. Terzoni, Micropor. Mespor. Mater. 6 (1996) 395–404.

[5] M. Niwa, K. Suzuki, N. Katada, T. Kanougi, T. Atoguchi, J. Phys. Chem. B 109 (2005) 18749–

18757.

[6] P.R.H.P. Rao, M. Matsukata, Chem. Commun. (1996) 1441–1442.

[7] M. Niwa, S. Nishikawa, N. Katada, Micropor. Mesopor. Mater. 82 (2005) 105–112.

[8] N. Katada, H. Tamagawa, M. Niwa, Catal. Today 226 (2014) 37-46.

[9] M. Niwa, N. Katada, K. Okumura, Characterization and Design of Zeolite Catalysts: Solid Acidity, Shape Selectivity and Loading Properties; Springer, Berlin, 2010.

[10] A. Auroux, Top. Catal. 19 (2002) 205–213.

[11] F. Lonyi, A. Kovacs, J. Valyon, J. Phys. Chem. B 110 (2006) 1711–1721.

[12] S. Walspurger, Y. Sun, A.S.S. Sido, J. Sommer, J. Phys. Chem. B 110 (2006) 18368–18373.

[13] N. Katada, K. Suzuki, T. Noda, W. Miyatani, F. Taniguchi, M. Niwa, Appl. Catal. A: Gen. 373 (2010) 208–213.

[14] A. Corma, V. Fornes, S.B. Pergher, Th.L.M. Maesen, J.G. Buglass, Nature 396 (1998) 353–356.

[15] S. Inagaki, T. Tatsumi, Chem. Commun. (2009) 2583–2585.

[16] G. Busca, Chem. Rev. 107 (2007) 5366–5410.

[17] K. Suzuki, N. Katada, M. Niwa, J. Phys. Chem. C 111 (2007) 894–900.

[18] K. Suzuki, T. Noda, G. Sastre, N. Katada, M. Niwa, J. Phys. Chem. C 113 (2009) 5672–5680.

[19] B. Xie, J.W. Song, L.M. Ren, Y.Y. Ji, J.X. Li, F.-S. Xiao, Chem. Mater. 20 (2008) 4533–4535.

[20] B. Xie, H. Zhang, C. Yang, S. Liu, L. Ren, L. Zhang, X. Meng, B. Yilmaz, U. Müller, F.-S. Xiao, Chem. Commun. 47 (2011) 3945–3947.

[21] G. Majano, L. Delmotte, V. Valtchev, S. Mintova, Chem. Mater. 21 (2009) 4184–4191.

[22] Y. Kamimura, W. Chaikittisip, K. Itabashi, A. Shimojima, T. Okubo, Chem.-Asian J. 5 (2010) 2182–2191.

[23] E. Loeffler, U. Lohse, Ch. Peuker, G. Oehlmann, L.M. Kustov, V.L. Zholobenko, V.B. Kazansky, Zeolites 10 (1990) 266-271.

[24] E. Bourgeat-Lami, P. Massiani, F.D. Renzo, P. Espiau, F. Fajula, Appl. Catal. 72 (1991) 139-152.

[25] K. Nakamoto, Infrared and Raman Spectra of Inorganic and Coordination Compounds, 6th Edition, Part B; John Wiley & Sons, Hoboken, 2009, p. 194.

[26] K. Nakamoto, Infrared and Raman Spectra of Inorganic and Coordination Compounds, 6th Edition, Part A; John Wiley & Sons, Hoboken, 2009, p. 3.

[27] W.L. Earl, P.O. Fritz, A.A.V. Gibson, J.H. Lunsford, J. Phys. Chem. 91 (1987) 2091–2095.

[28] F. Lónyi, J. Valyon, Thermochim. Acta 373 (2001) 53–57.

[29] A. Zecchina, L. Marchese, S. Bordiga, C. Pazé, E. Gianotti, J. Phys. Chem. B 101 (1997) 10128–10135.

[30] N. Katada, T. Tsubaki, M. Niwa, Appl. Catal. A: Gen. 340 (2008) 76–86.

[31] H. Zhang, B. Xie, X. Meng, U. Müller, B. Yilmaz, M. Feyen, S. Maurer, H. Gies, T. Tatsumi, X. Bao, W. Zhang, D.D. Vos, F.S. Xiao, Micropor. Mesopor. Mater. 180 (2013) 123-129.

[32] N. Katada, H. Igi, J.-H. Kim, M. Niwa, J. Phys. Chem. B 101 (1997) 5969–5977.

[33] J.C. Jansen, E.J. Creyghton, S.L. Njo, H. van Koningsveld, H. van Bekkum, Catal. Today 38 (1997) 205–212.

[34] C. Jia, P. Massani, D.J. Barthomeuf, Chem. Soc. Faraday Trans. 89 (1993) 3659–3665.

[35] N. Katada, S. Iijima, H. Igi, M. Niwa, Stud. Surf. Sci. Catal. 105 (1996) 1227–1234.

[36] Y. Miyamoto, N. Katada, M. Niwa, Micropor. Mesopor. Mater. 40 (2000) 271–281.

[37] N. Katada, K. Suzuki, T. Noda, G. Sastre, M. Niwa, J. Phys. Chem. C 113 (2009) 19208–19217.

[38] F. Collignon, R. Loenders, J.A. Martens, P.A. Jacobs, G. Poncelet, G. J. Catal. 182 (1999) 302–312.

[39] F. Collignon, G. Poncelet, J. Catal. 202 (2001) 68–77.

[40] M. Niwa, N. Katada, N.; Catal. Surveys Jpn. 1 (1997) 215–226.

Table 1: Determined parameters showing the acidic property

Sample	Si/Al	Al concentration [Al] / mol kg^{-1}	Number of Brønsted acid sites [B_{as}] / mol kg^{-1}	Number of Lewis acid sites [L_{as}] / mol kg^{-1}	[B_{as}] / [Al] / %
SDS-BEA	5.3	2.65	0.67	0.15	25
cntl-BEA	5.3	2.65	0.37	0.08	14
JRC-Z-B25	12.5	1.23	0.53	0.05	43

Figure captions

Figure 1: IR spectra in a region of 3300 - 3800 cm^{-1} on (A) SDS-BEA, (B) cntl-BEA, and (C) JRC-Z-B25 measured at 373 K after pretreatment at 823 K.

Figure 2: Difference spectra of IR $A(T)$-$N(T)$ [(spectrum after ammonia adsorption) - (spectrum before ammonia adsorption)] on (A) SDS-BEA, (B) cntl-BEA, and (C) JRC-Z-B25.

Figure 3: Enlarged portion at -OH stretching vibration region (3450 - 3820 cm^{-1}) of Figure 2 on (A) SDS-BEA, (B) cntl-BEA, and (C) JRC-Z-B25. The baseline for each of these spectra was corrected.

Figure 4: Enlarged portion at bending vibration region (1100 - 2000 cm^{-1}) of Figure 2 on (A) SDS-BEA, (B) cntl-BEA, and (C) JRC-Z-B25.

Figure 5: Vibration modes of 1450 (A, NH_4) and 1300 cm^{-1}-bands (B, NH_3). The symbols ○, ● and ⊘ show H, N and metal (Lewis acid site) atoms, respectively.

Figure 6: Examples of deconvolution of bending vibration region of IR spectrum. (A) and (B): SDS-BEA, (C) and (D): cntl-BEA, (E) and (F): JRC-Z-B25, (A), (C) and (E): 373 K, (B), (D), and (F): 523 K.

Figure 7: Fitting of IR- and MS-TPD giving TPD spectra of Brønsted and Lewis acid sites on (A) SDS-BEA, (B) cntl-BEA, and (C) JRC-Z-B25.

Figure 8: Curve fitting for determination of strength distribution on (A) SDS-BEA, (B) cntl-BEA, and (C) JRC-Z-B25.

Figure 9: Strength distribution of Brønsted acid sites.

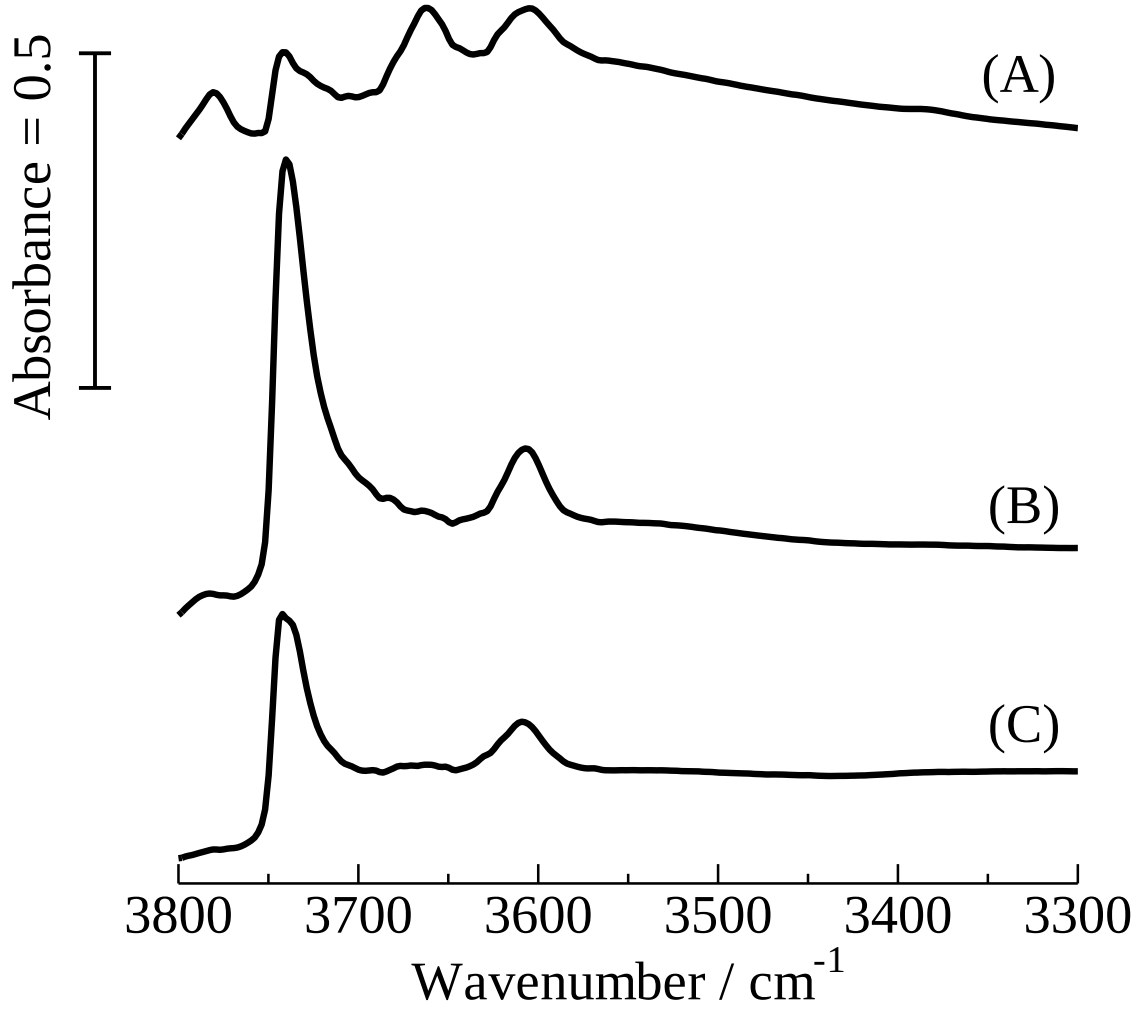
Absorbance = 0.5
(A)
(B)
(C)
3800
3700
3600
3500
3400
3300
Wavenumber / cm-1

Figure 1

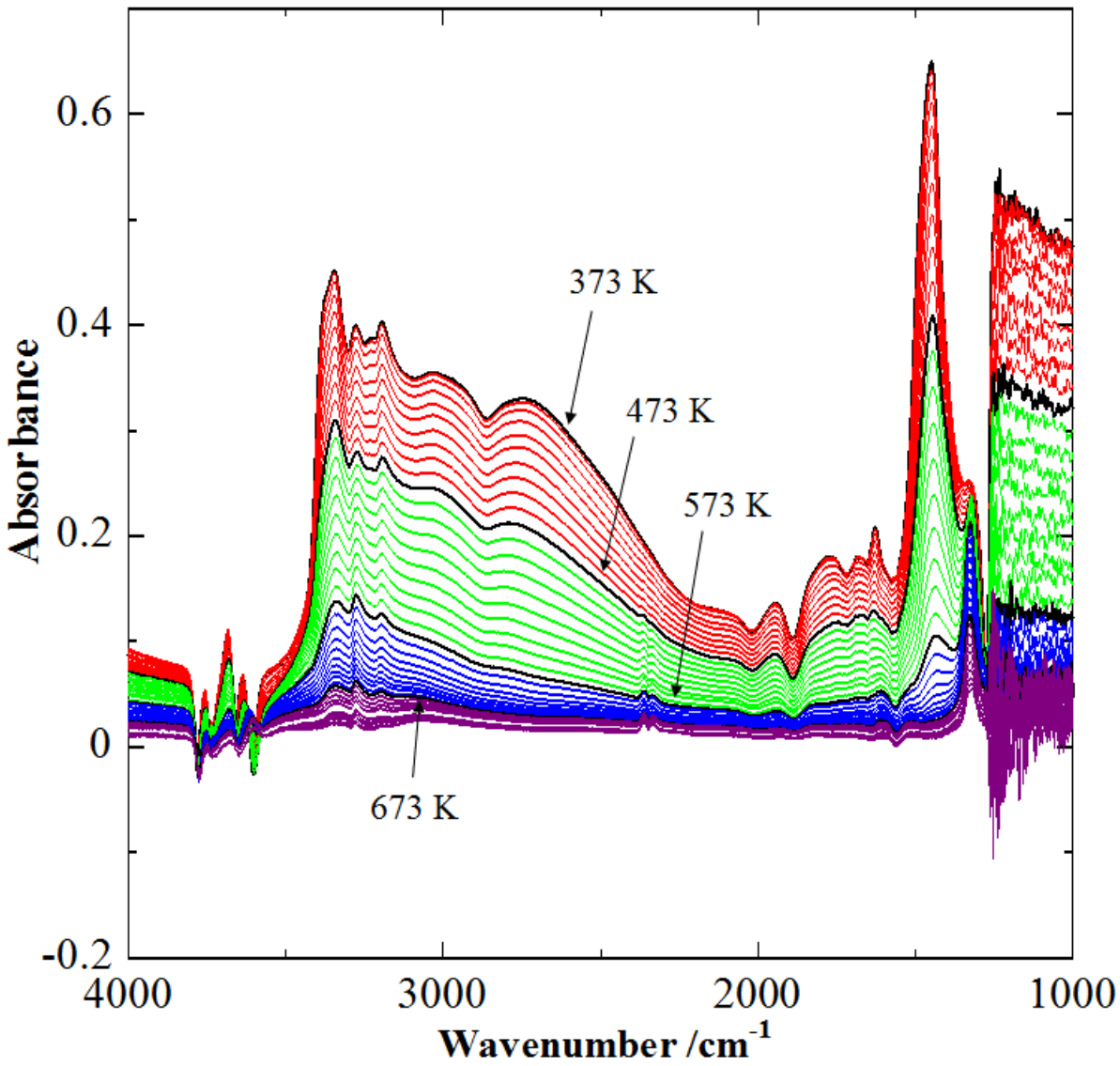
0.6
0.4
0.2
0
-0.2
Absorbance
373 K
473 K
573 K
673 K
4000
3000
2000
1000
Wavenumber /cm-1

Figure 2 (A)

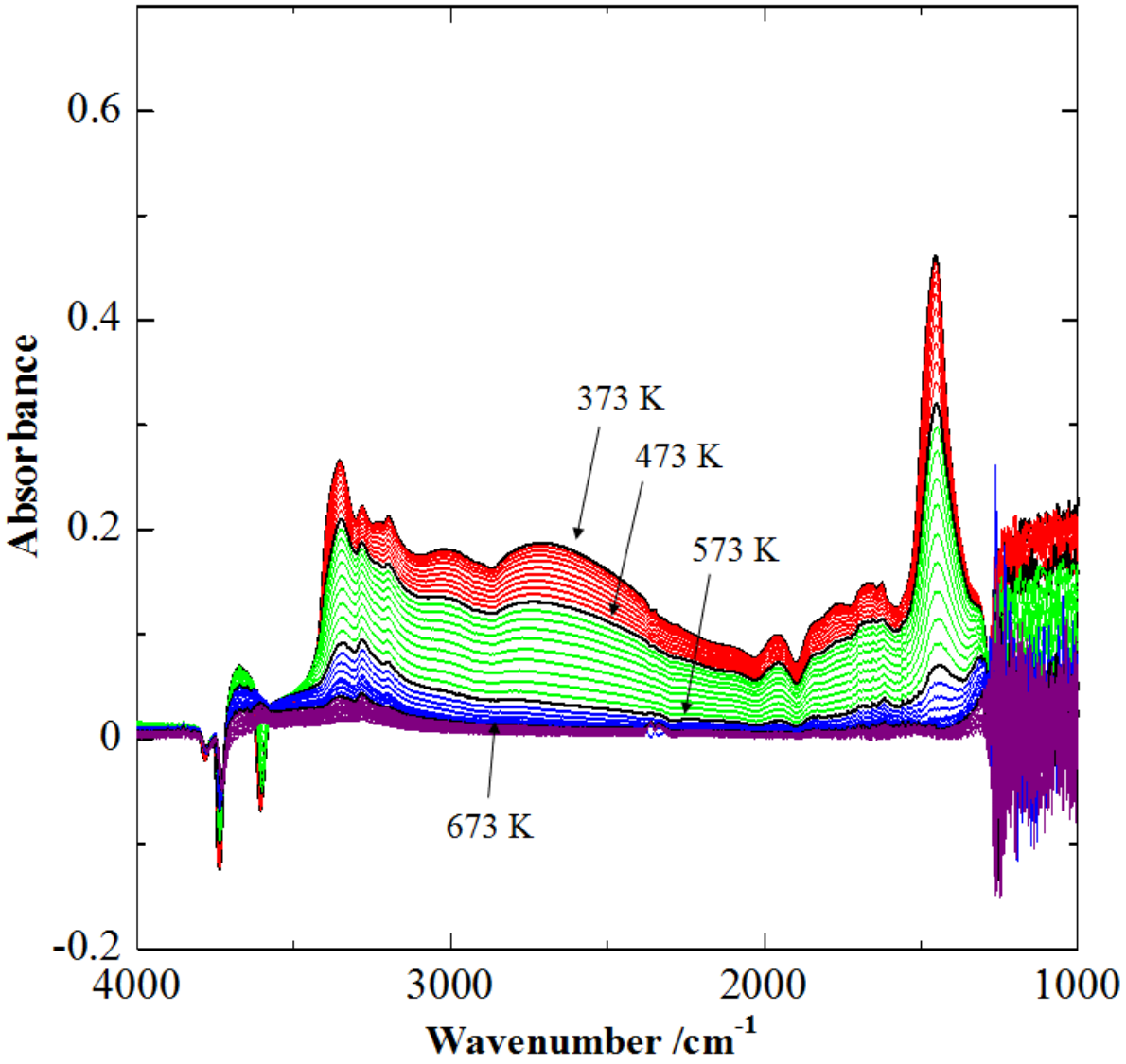
0.6
0.4
0.2
0
-0.2
Absorbance
373 K
473 K
573 K
673 K
4000
3000
2000
1000
Wavenumber /cm-1

Figure 2 (B)

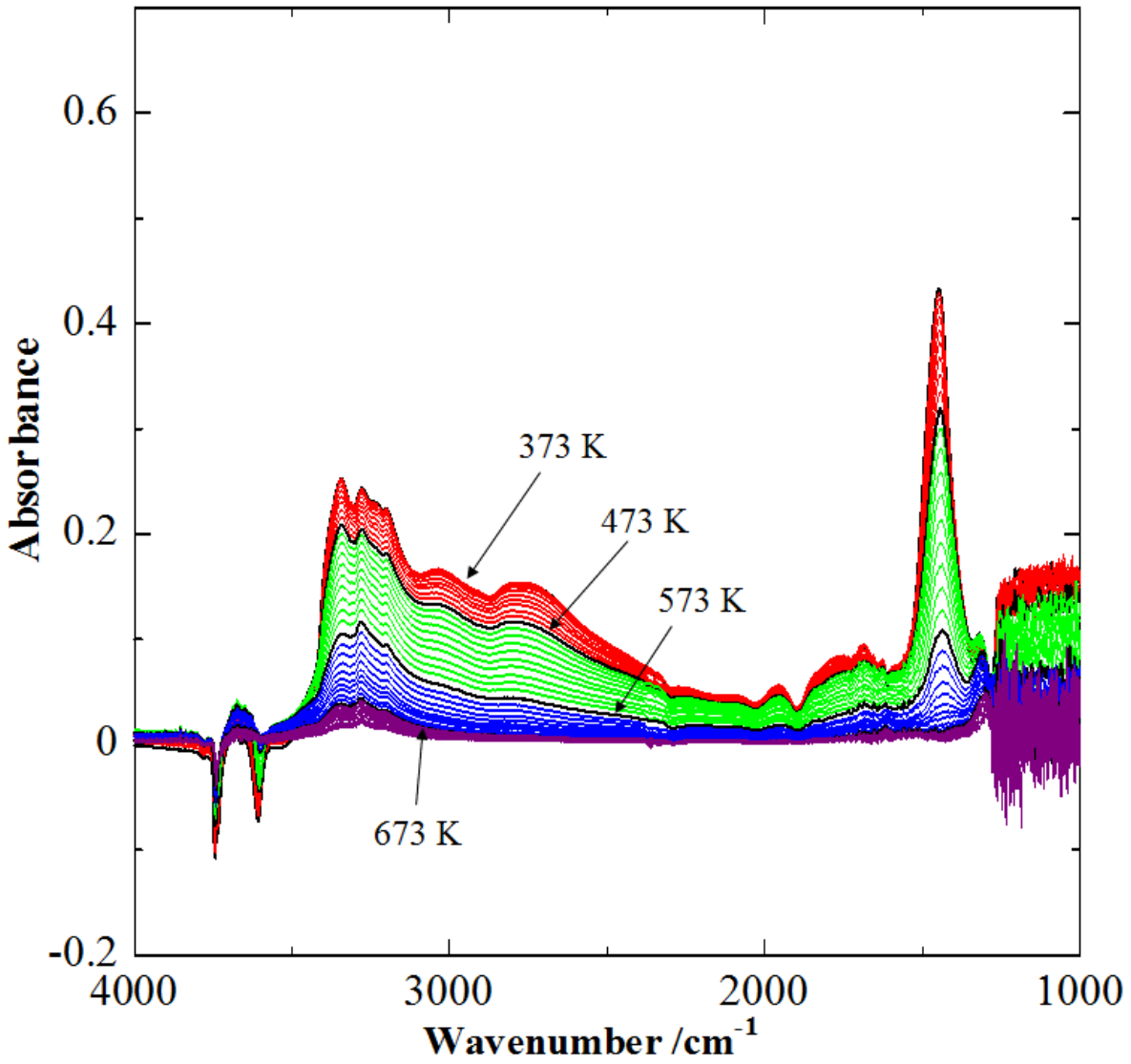
0.6
0.4
0.2
0
-0.2
Absorbance
373 K
473 K
573 K
673 K
4000
3000
2000
1000
Wavenumber /cm-1

Figure 2 (C)

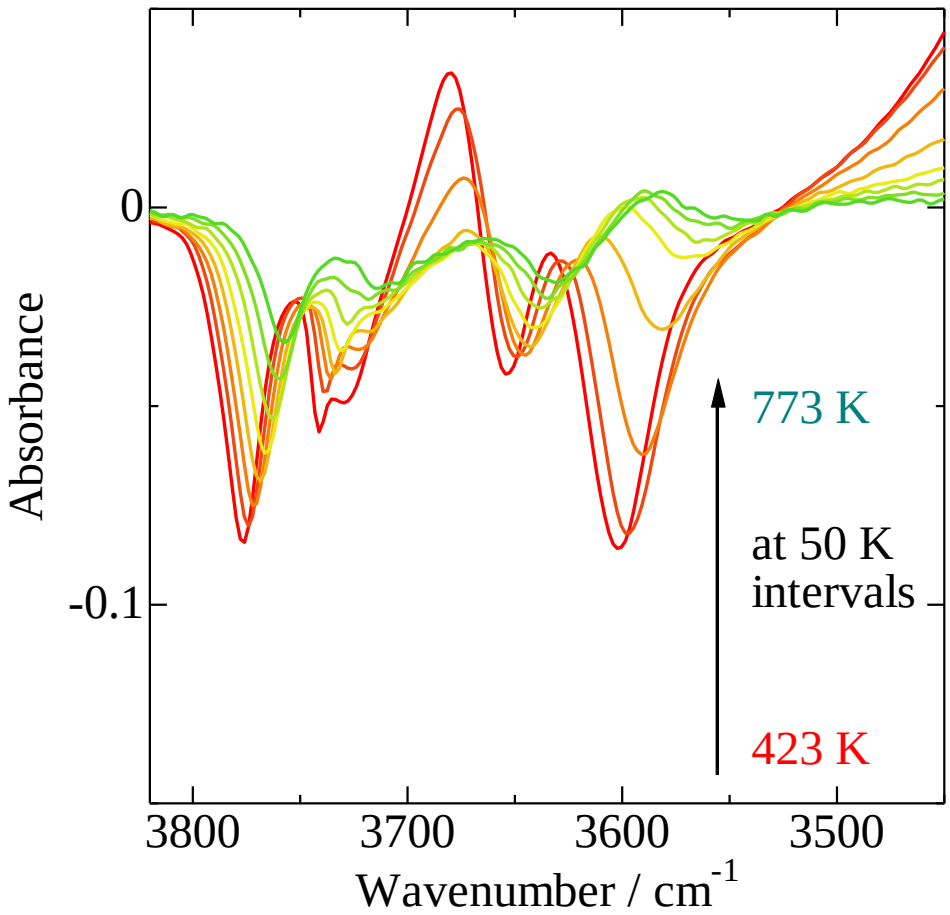
0
-0.1
Absorbance
773 K
at 50 K
intervals
423 K
3800
3700
3600
3500
Wavenumber / cm-1

Figure 3 (A)

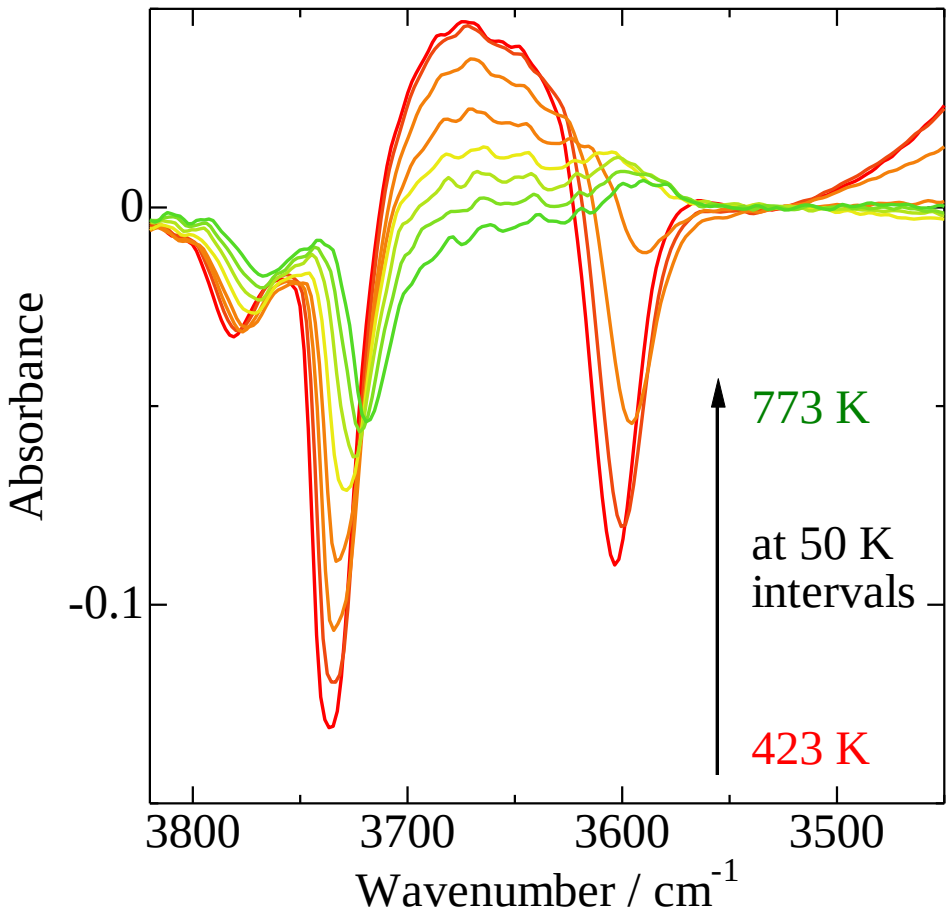
0
-0.1
Absorbance
773 K
at 50 K
intervals
423 K
3800
3700
3600
3500
Wavenumber / cm-1

Figure 3 (B)

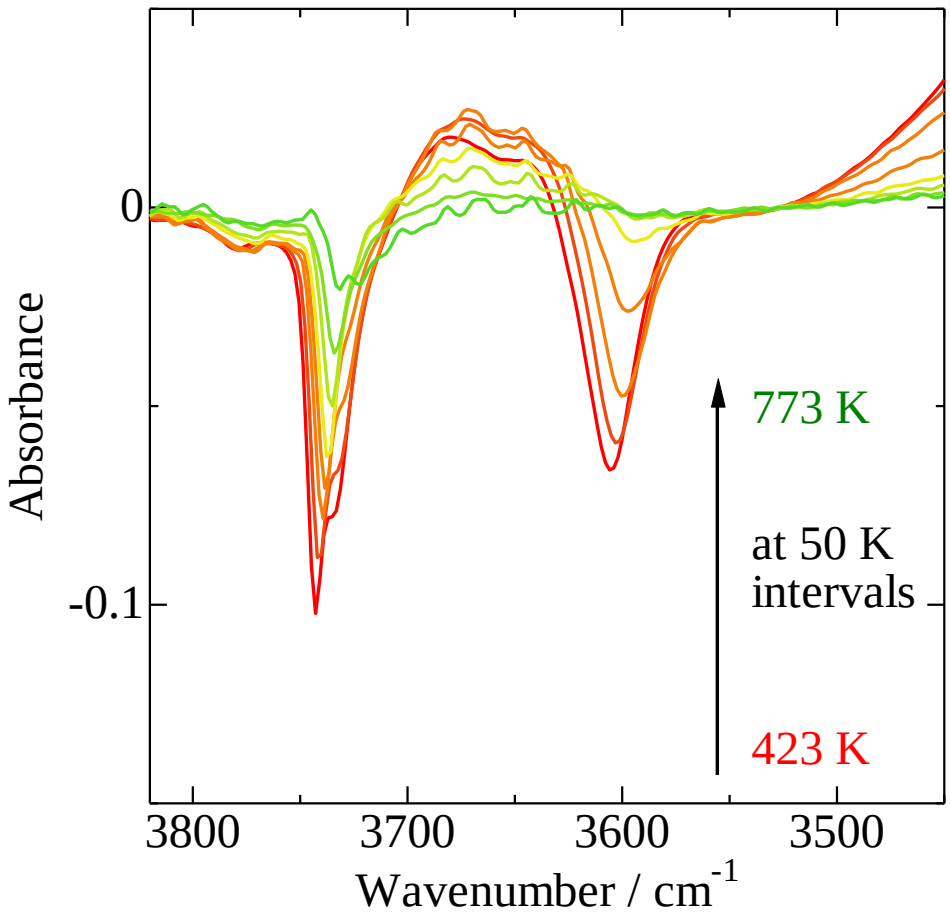
0
-0.1
Absorbance
773 K
at 50 K
intervals
423 K
3800
3700
3600
3500
Wavenumber / cm-1

Figure 3 (C)

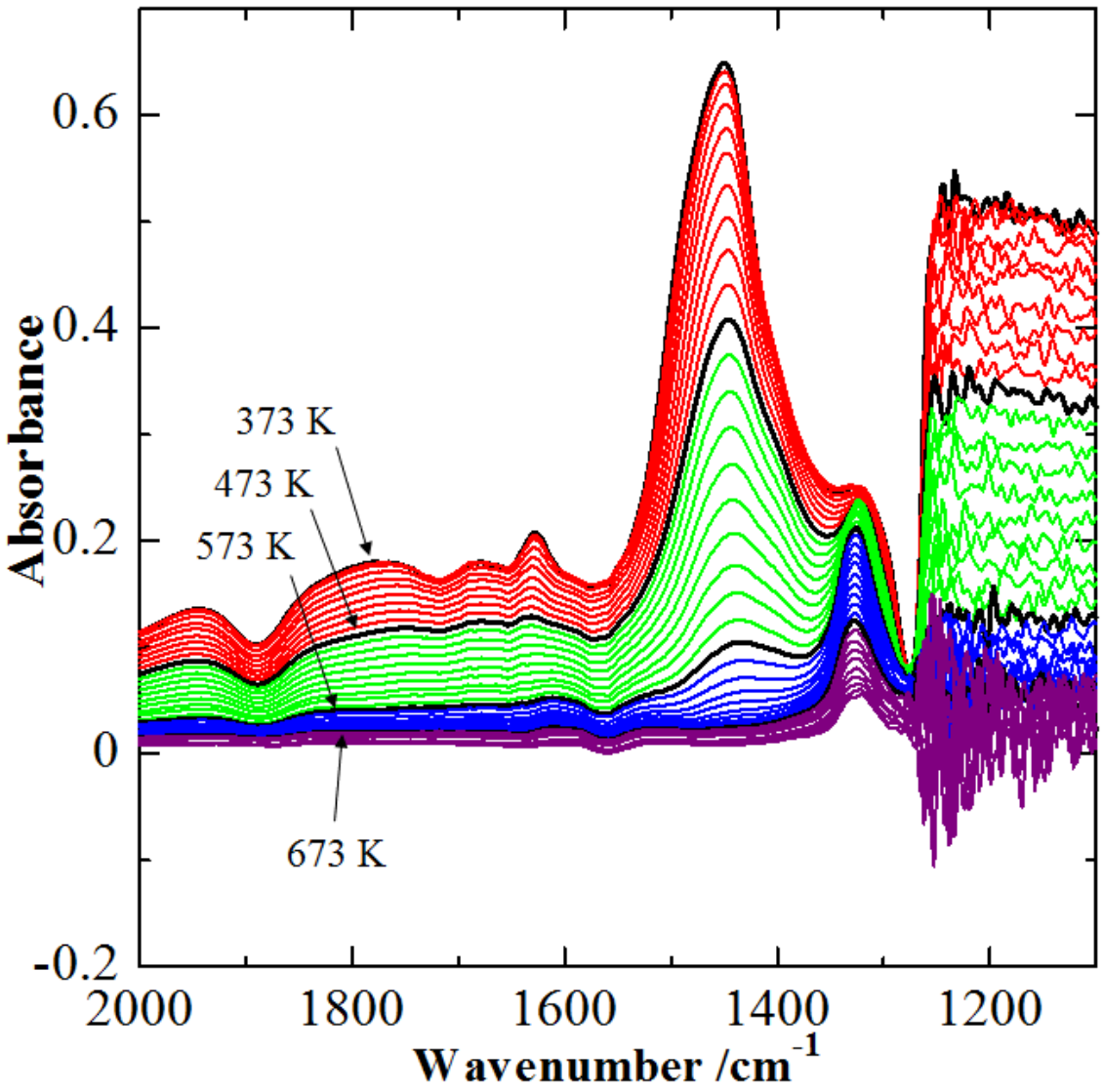
0.6
0.4
0.2
0
-0.2
Absorbance
373 K
473 K
573 K
673 K
2000
1800
1600
1400
1200
Wavenumber /cm-1

Figure 4 (A)

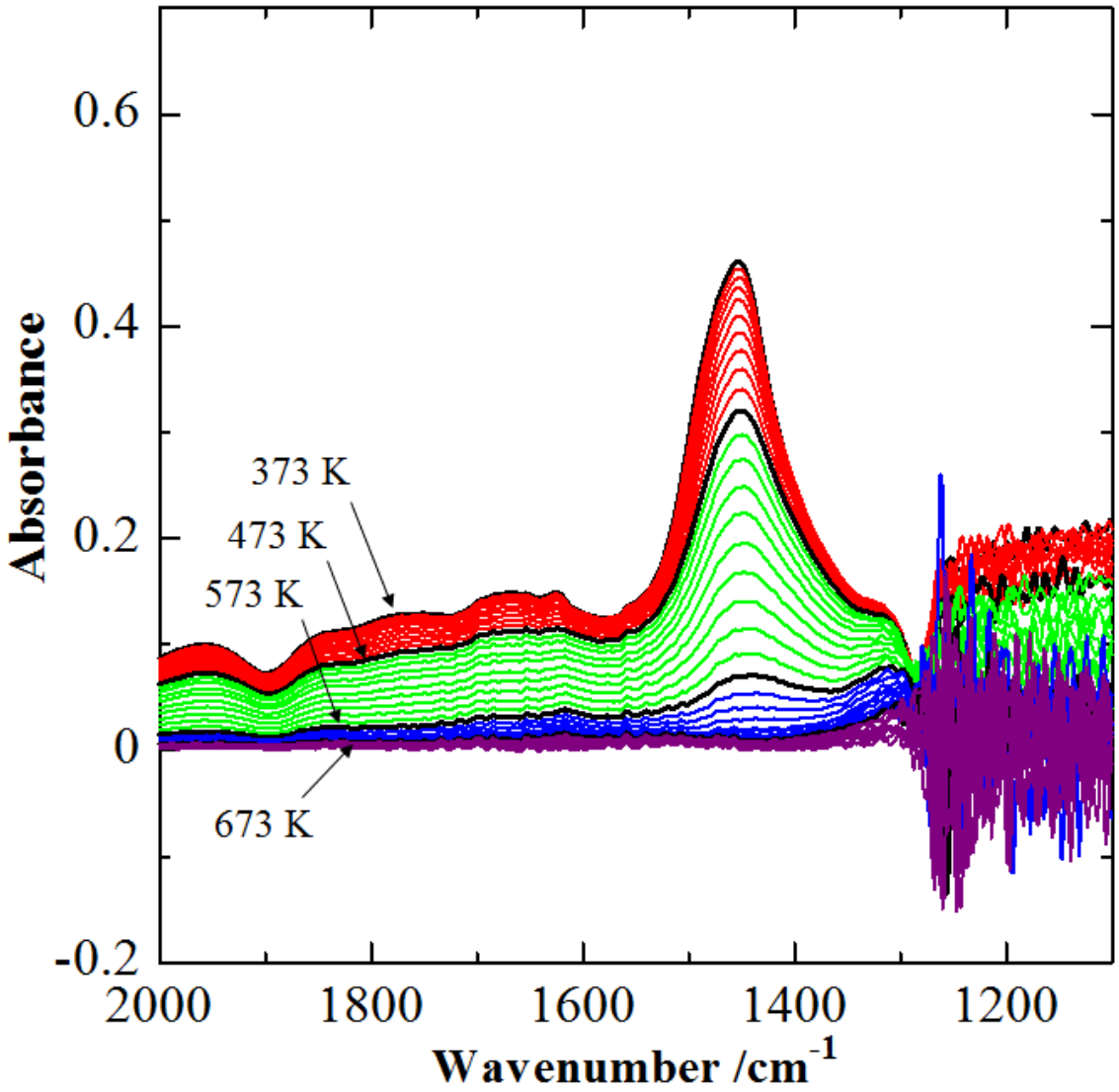
0.6
0.4
0.2
0
-0.2
Absorbance
373 K
473 K
573 K
673 K
2000
1800
1600
1400
1200
Wavenumber /cm-1

Figure 4 (B)

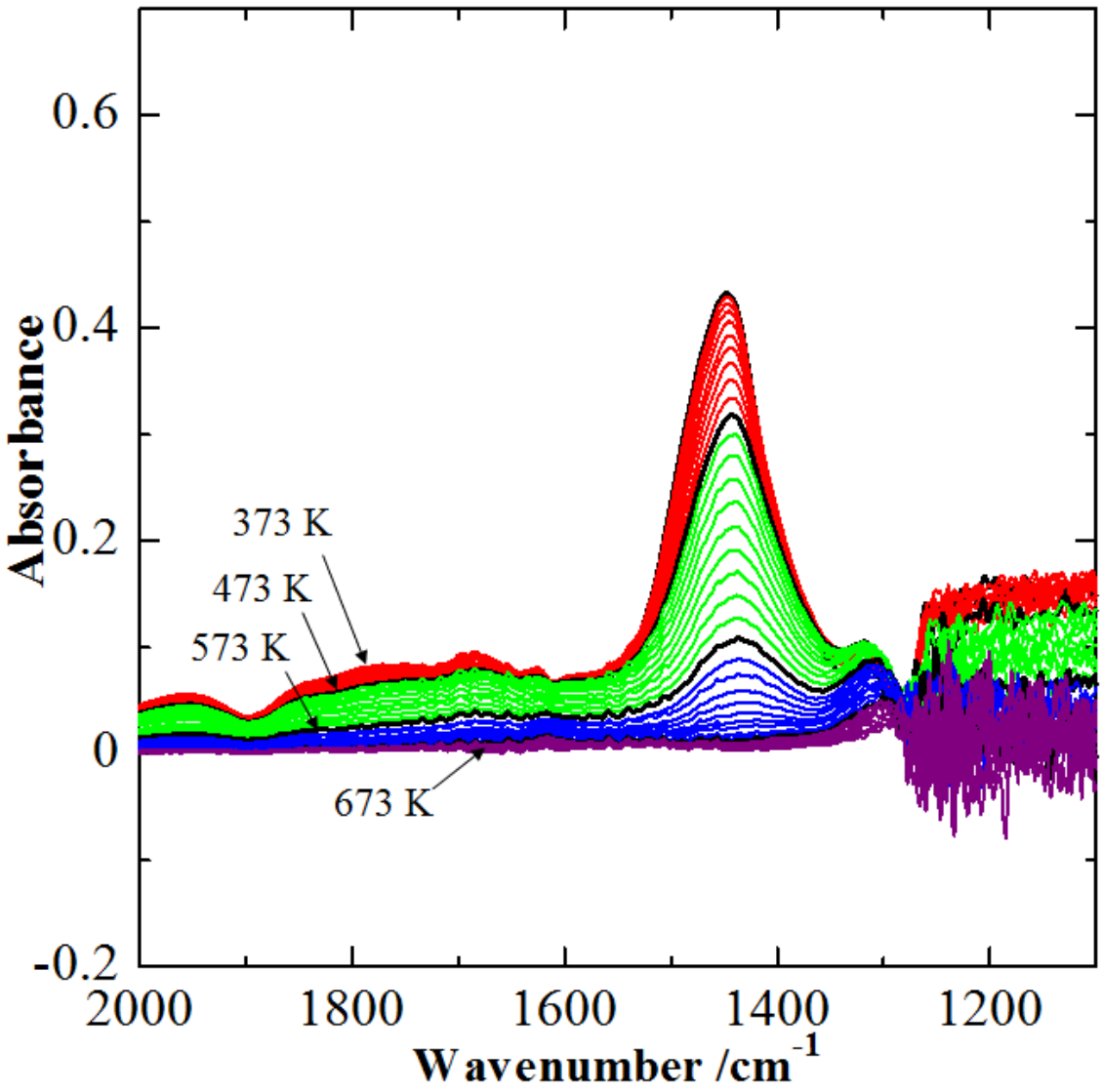
0.6
0.4
0.2
0
-0.2
Absorbance
373 K
473 K
573 K
673 K
2000
1800
1600
1400
1200
Wavenumber /cm-1

Figure 4 (C)

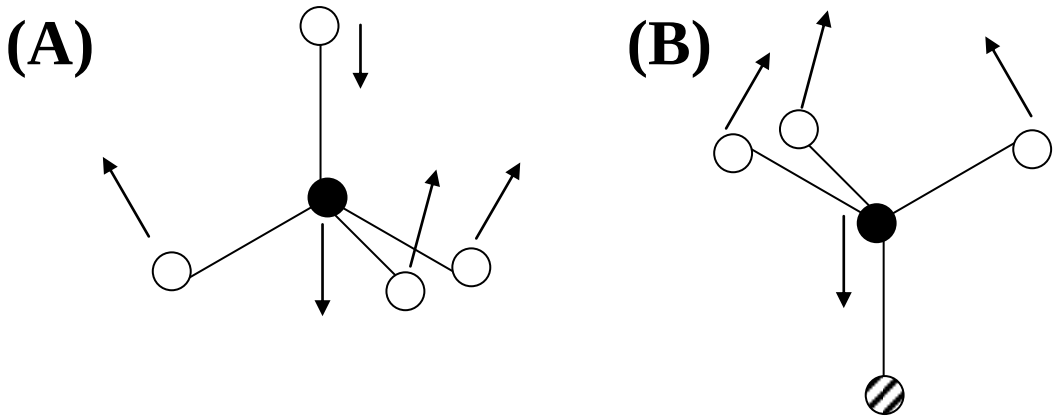

Figure 5

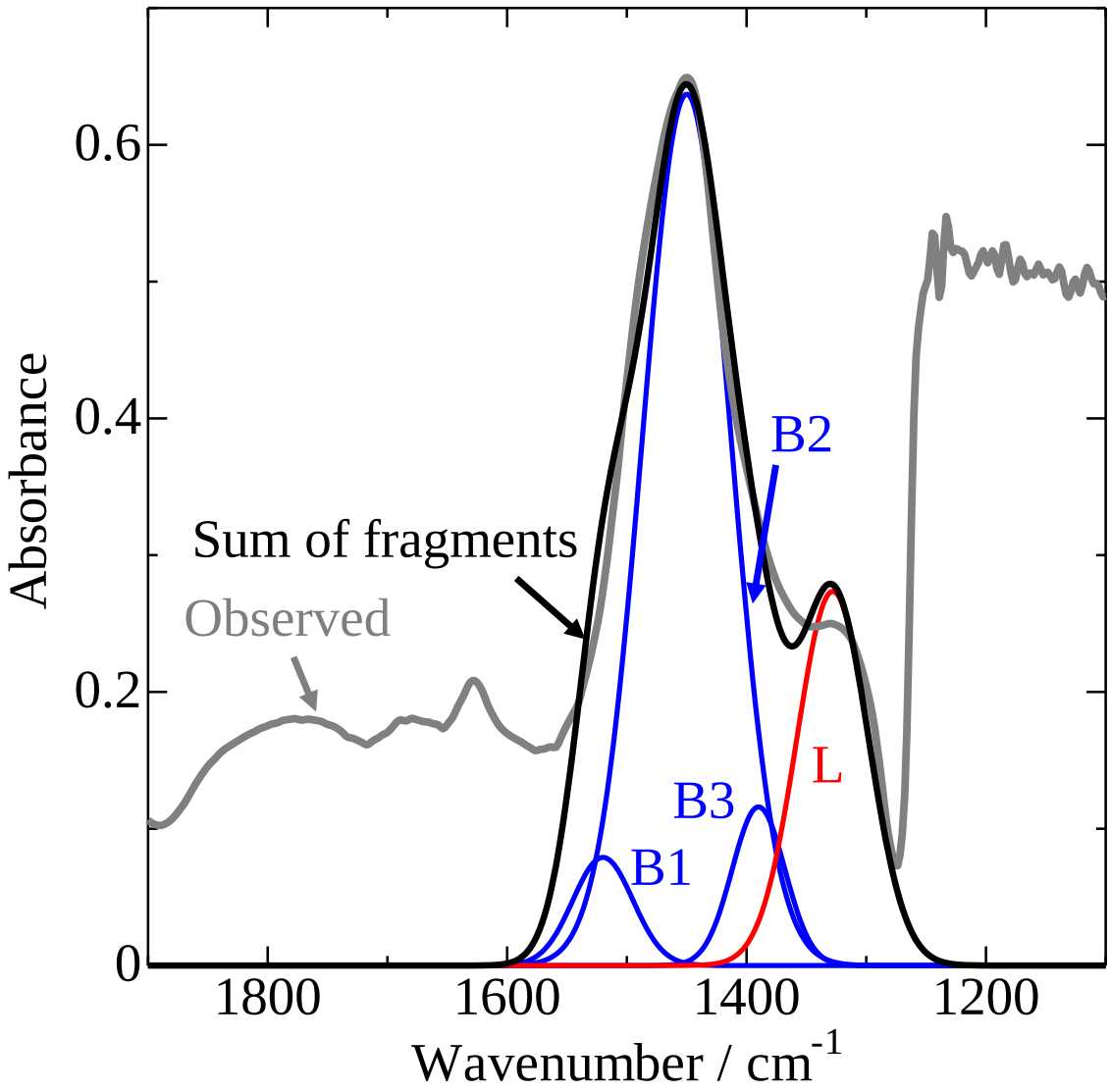
0.6
0.4
0.2
0
Absorbance
Sum of fragments
Observed
B2
B3
B1
L
1800
1600
1400
1200
Wavenumber / cm-1

Figure 6 (A)

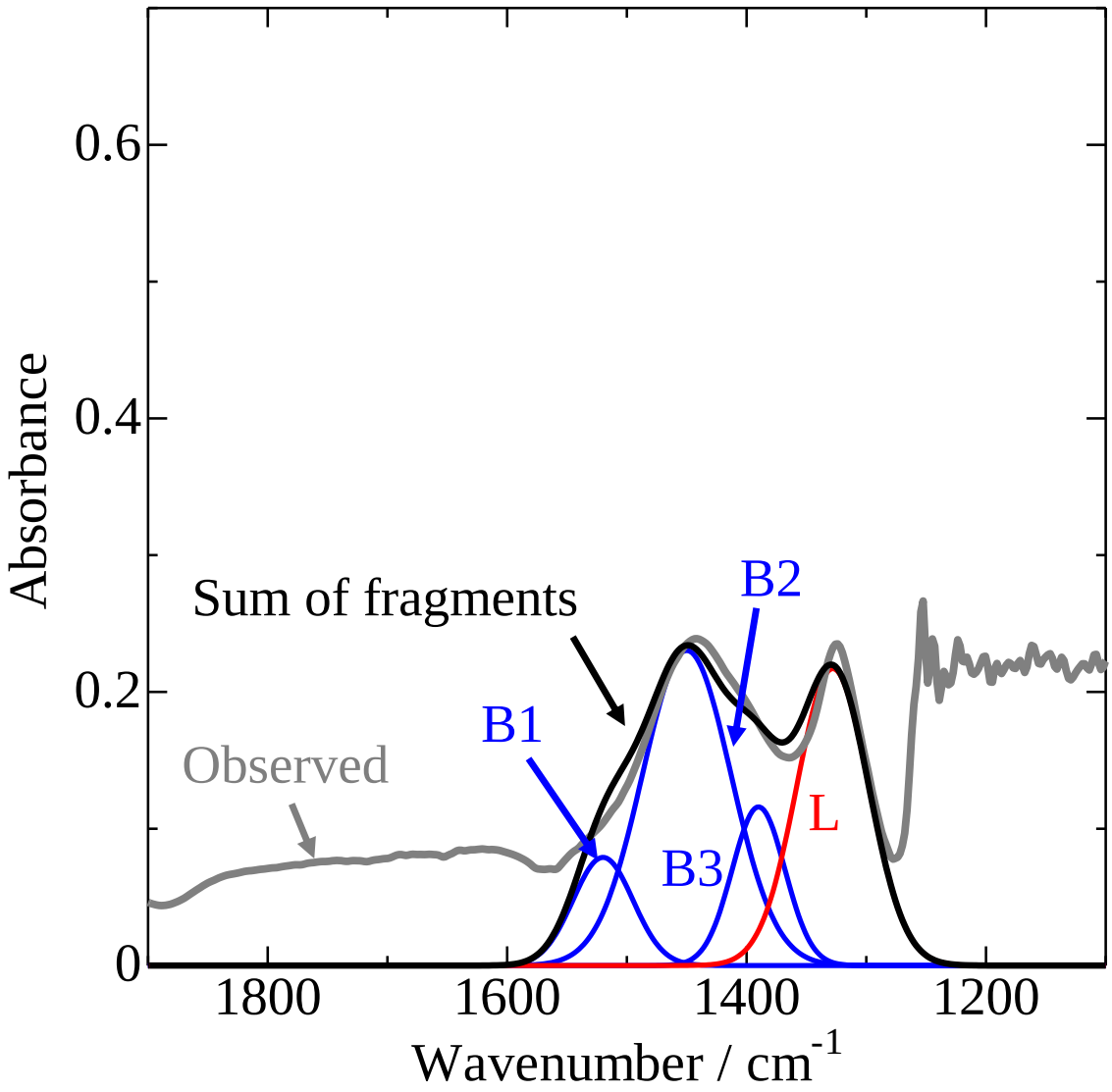
0.6
0.4
0.2
0
Absorbance
Sum of fragments
B2
B1
Observed
L
B3
1800
1600
1400
1200
Wavenumber / cm-1

Figure 6 (B)

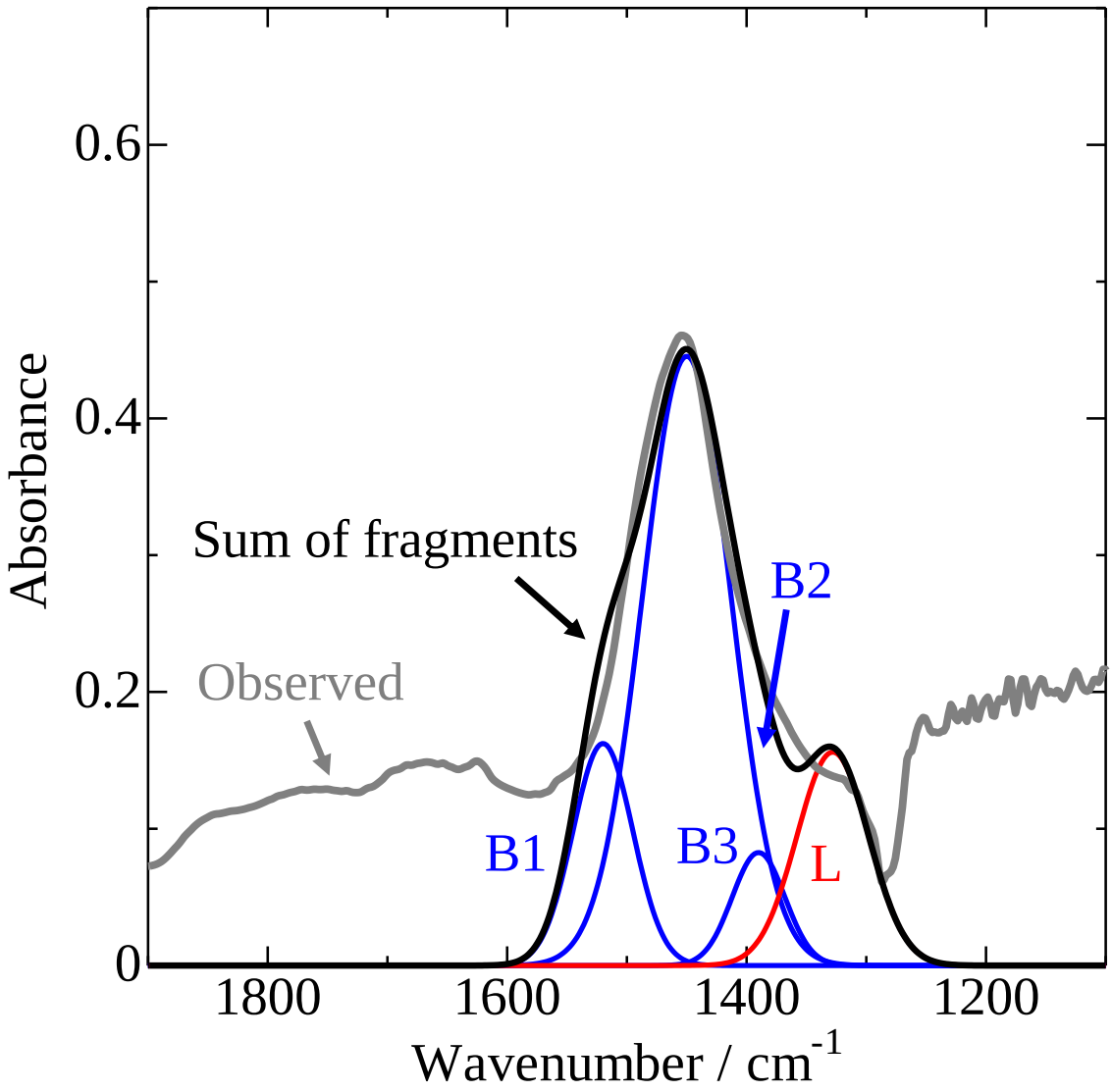
0.6
0.4
0.2
0
Absorbance
Sum of fragments
Observed
B1
B2
B3
L
1800
1600
1400
1200
Wavenumber / cm-1

Figure 6 (C)

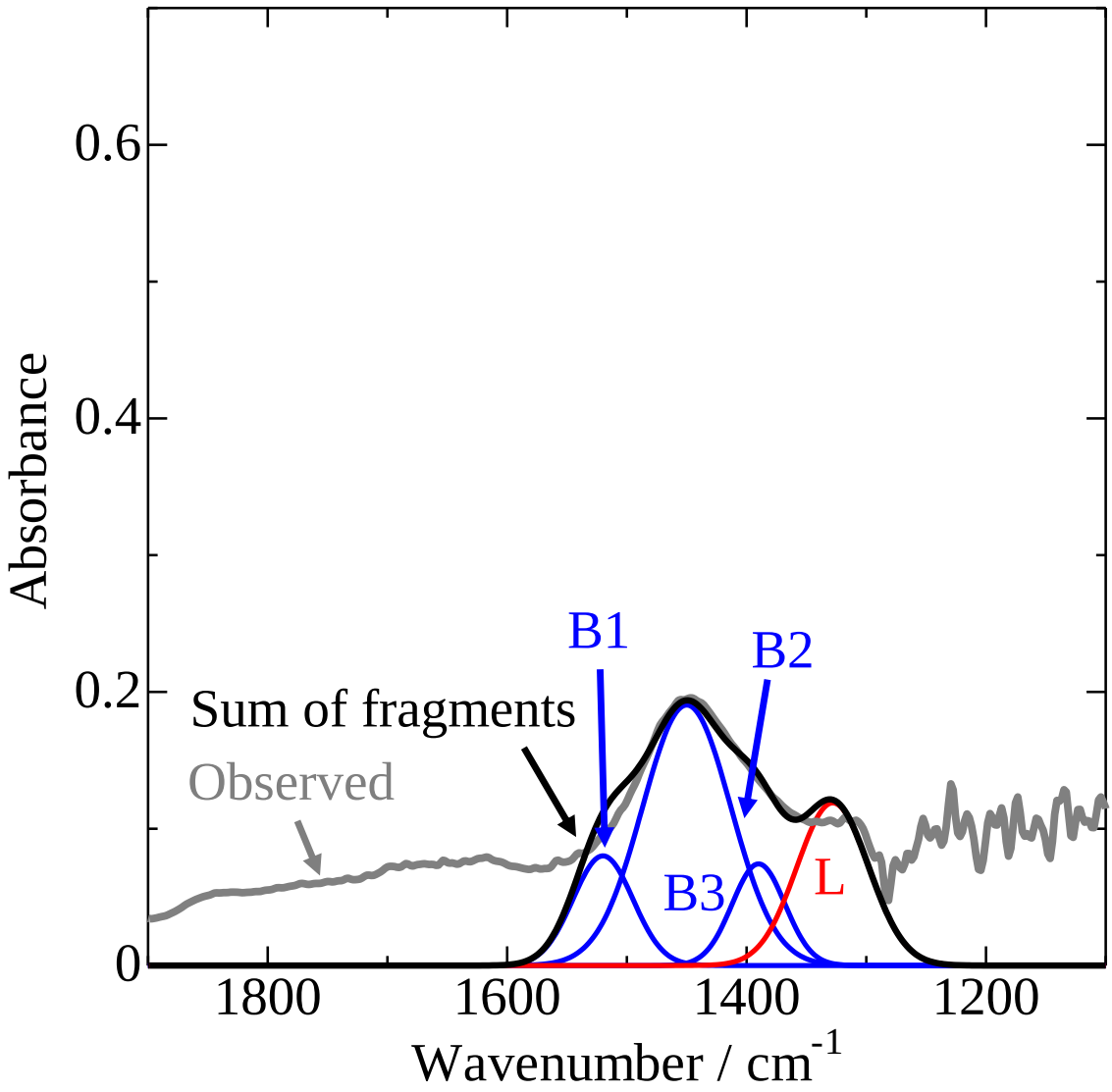
0.6
0.4
0.2
0
Absorbance
B1
B2
Sum of fragments
Observed
B3
L
1800
1600
1400
1200
Wavenumber / cm-1

Figure 6 (D)

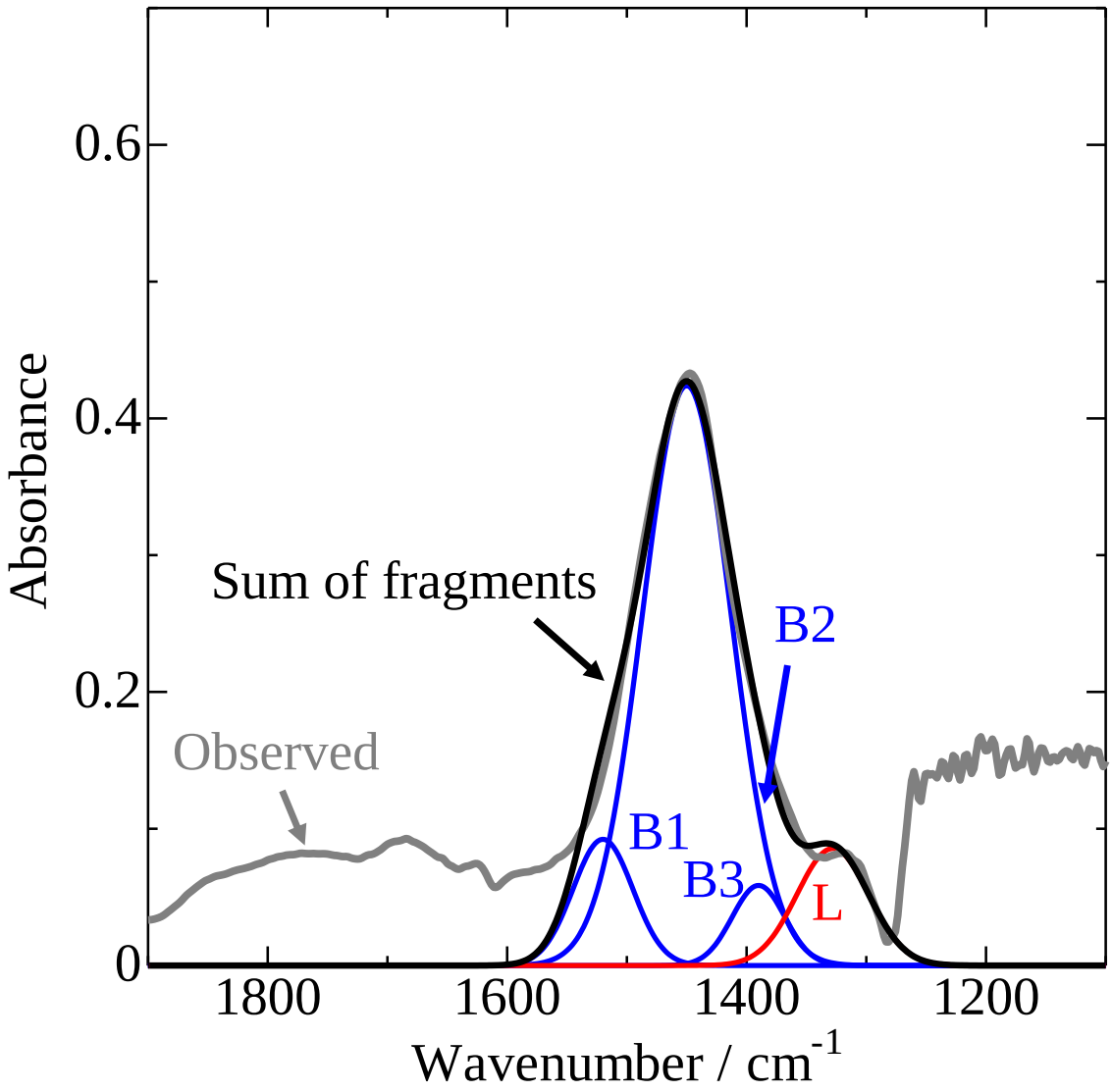
0.6
0.4
0.2
0
Absorbance
Sum of fragments
B2
Observed
B1
B3
L
1800
1600
1400
1200
Wavenumber / cm-1

Figure 6 (E)

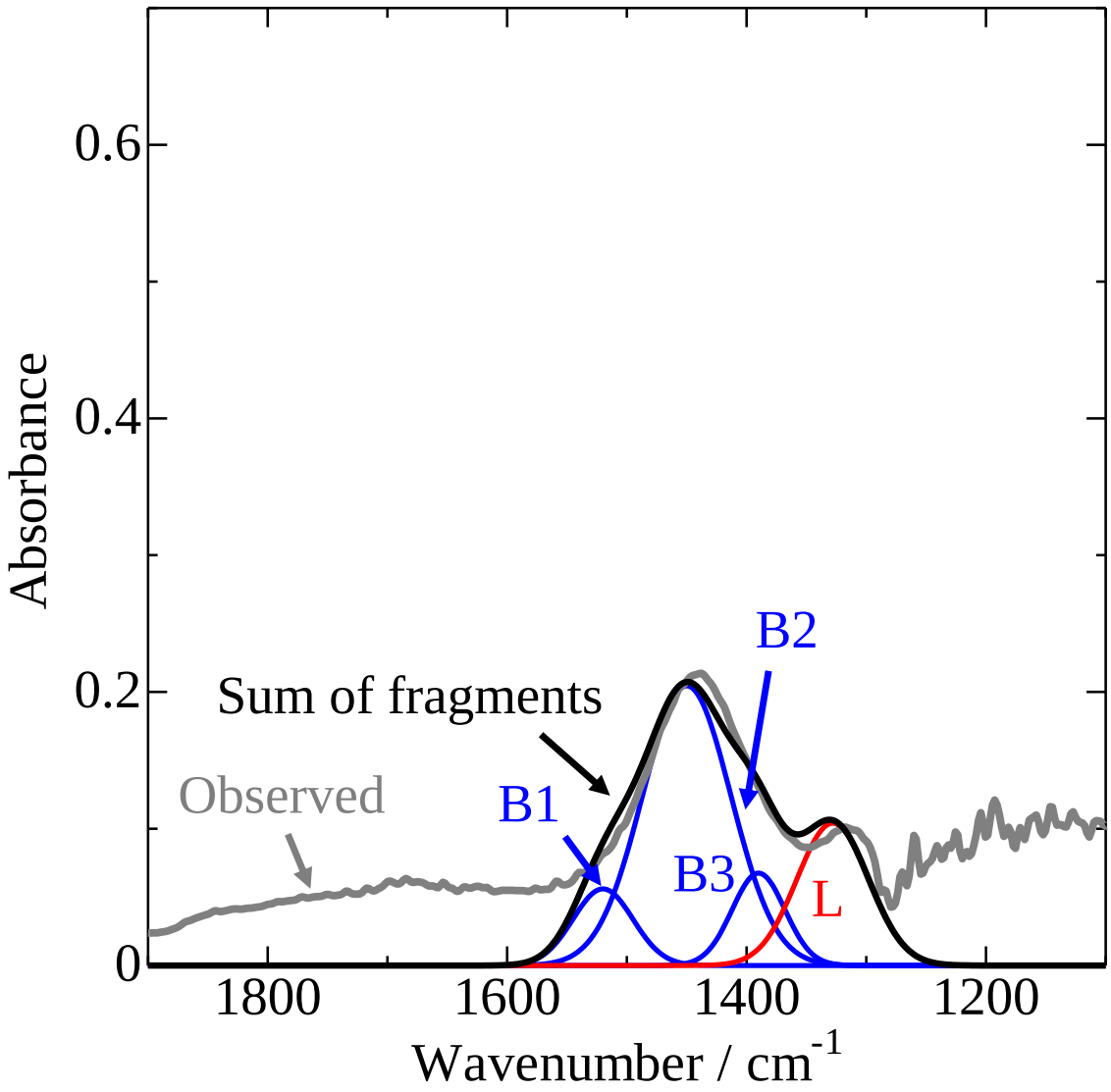
0.6
0.4
0.2
0
Absorbance
1800
1600
1400
1200
Wavenumber / cm-1
Sum of fragments
Observed
B1
B2
B3
L

Figure 6 (F)

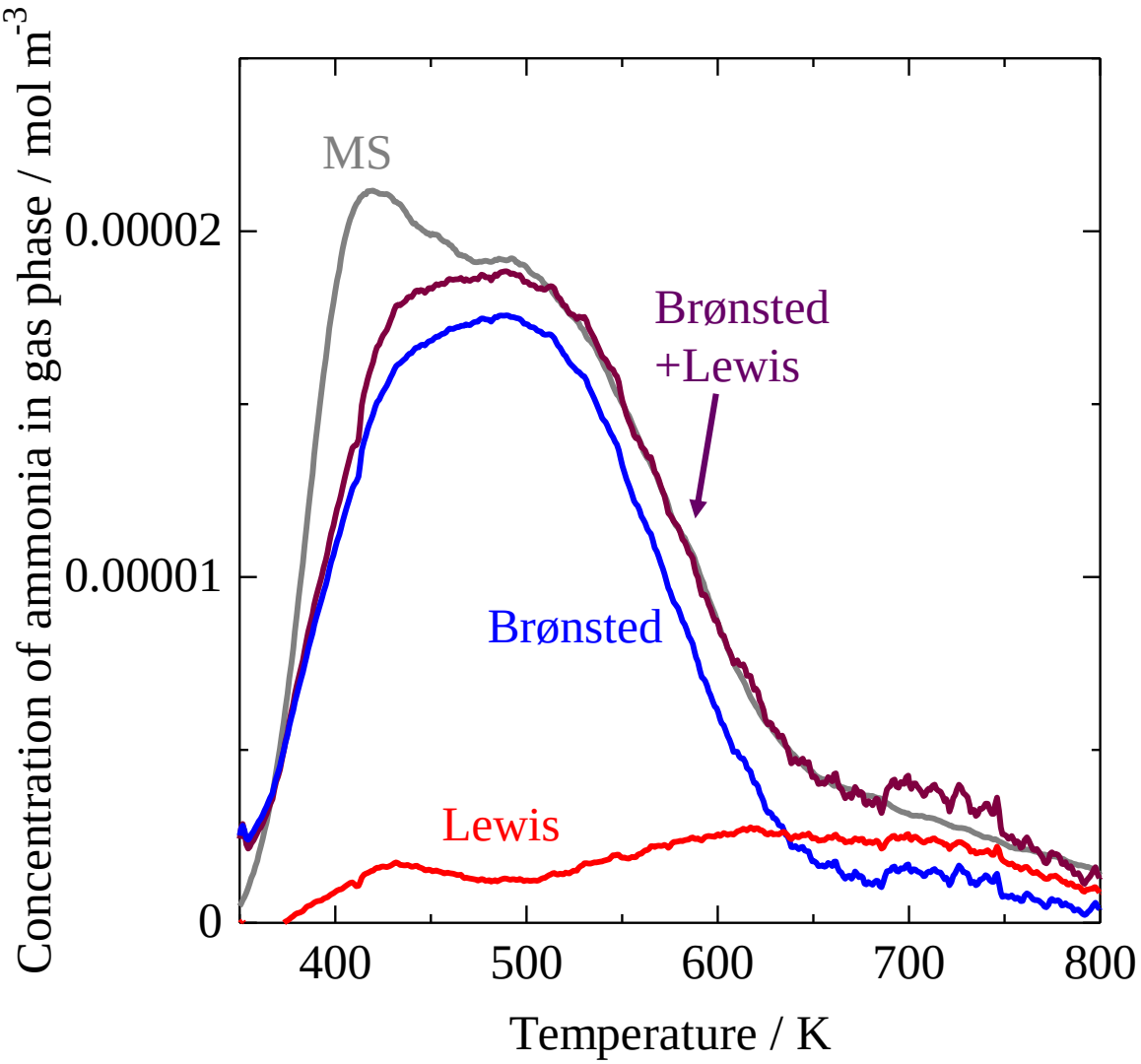
Concentration of ammonia in gas phase / mol m-3
0.00002
0.00001
0
MS
Brønsted
+Lewis
Brønsted
Lewis
400
500
600
700
800
Temperature / K

Figure 7 (A)

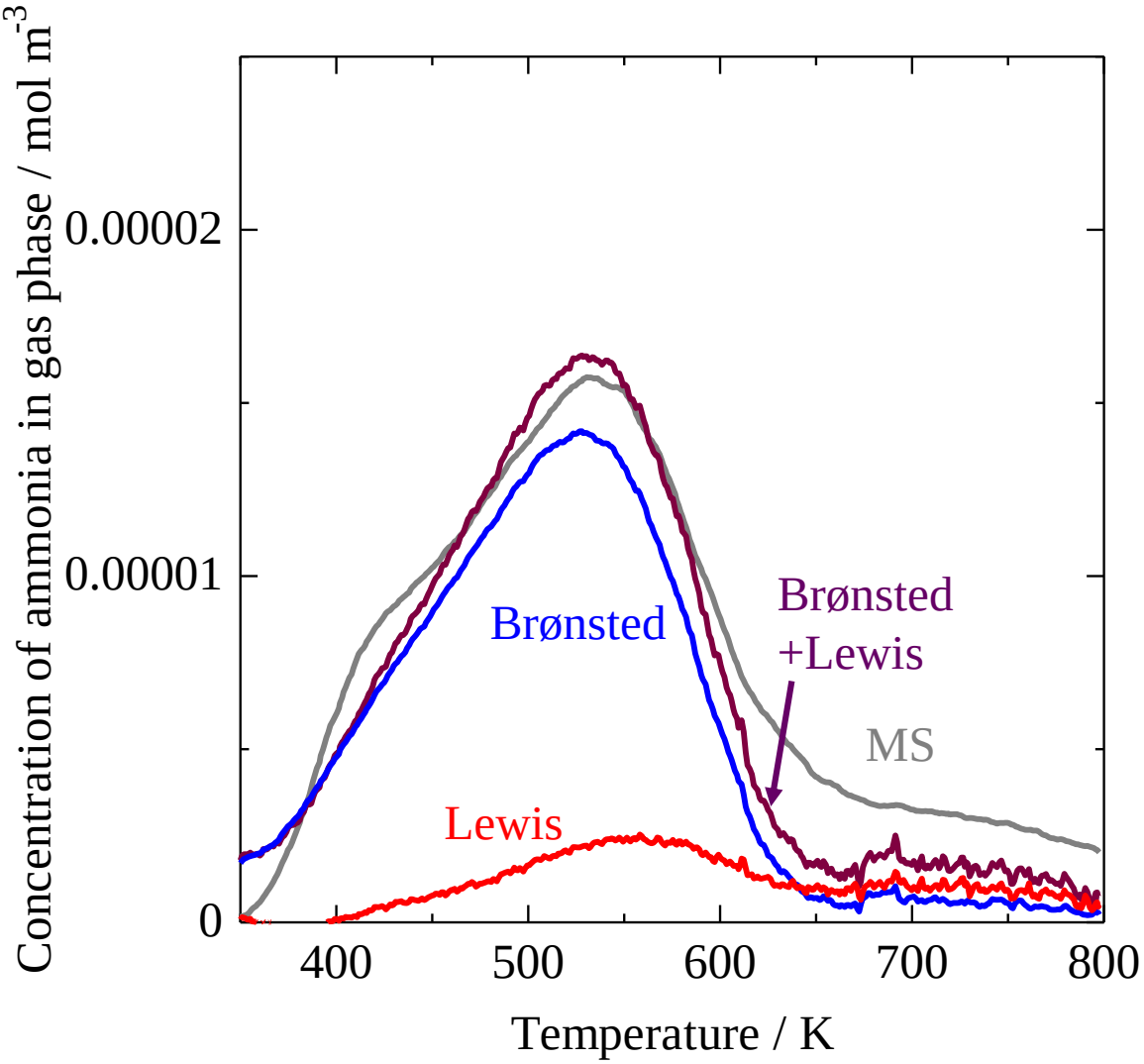
Concentration of ammonia in gas phase / mol m-3
0.00002
0.00001
0
400
500
600
700
800
Temperature / K
Brønsted
Brønsted
+Lewis
MS
Lewis

Figure 7 (B)

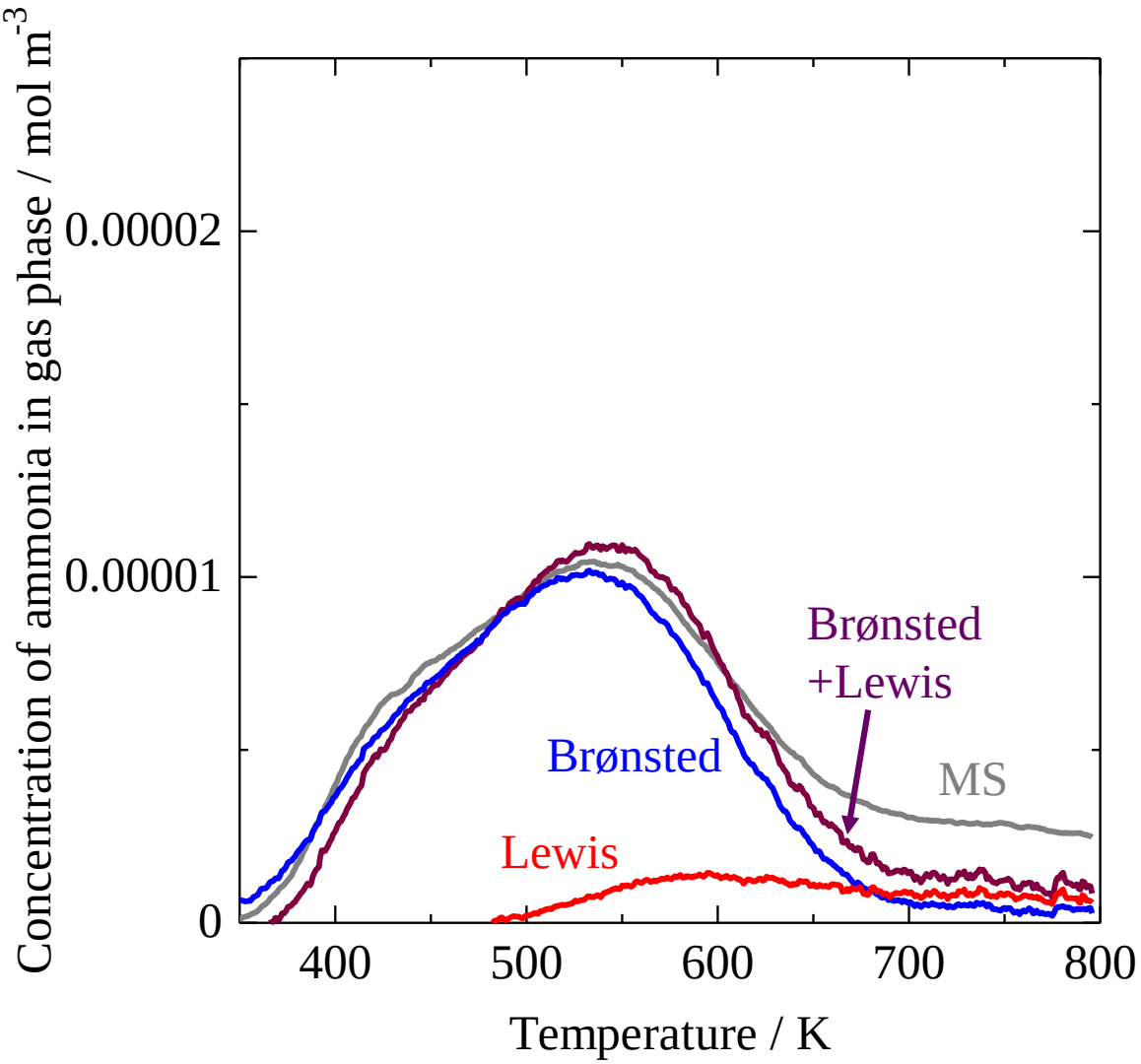
Concentration of ammonia in gas phase / mol m-3
0.00002
0.00001
0
400
500
600
700
800
Temperature / K
Brønsted
+Lewis
Brønsted
MS
Lewis

Figure 7 (C)

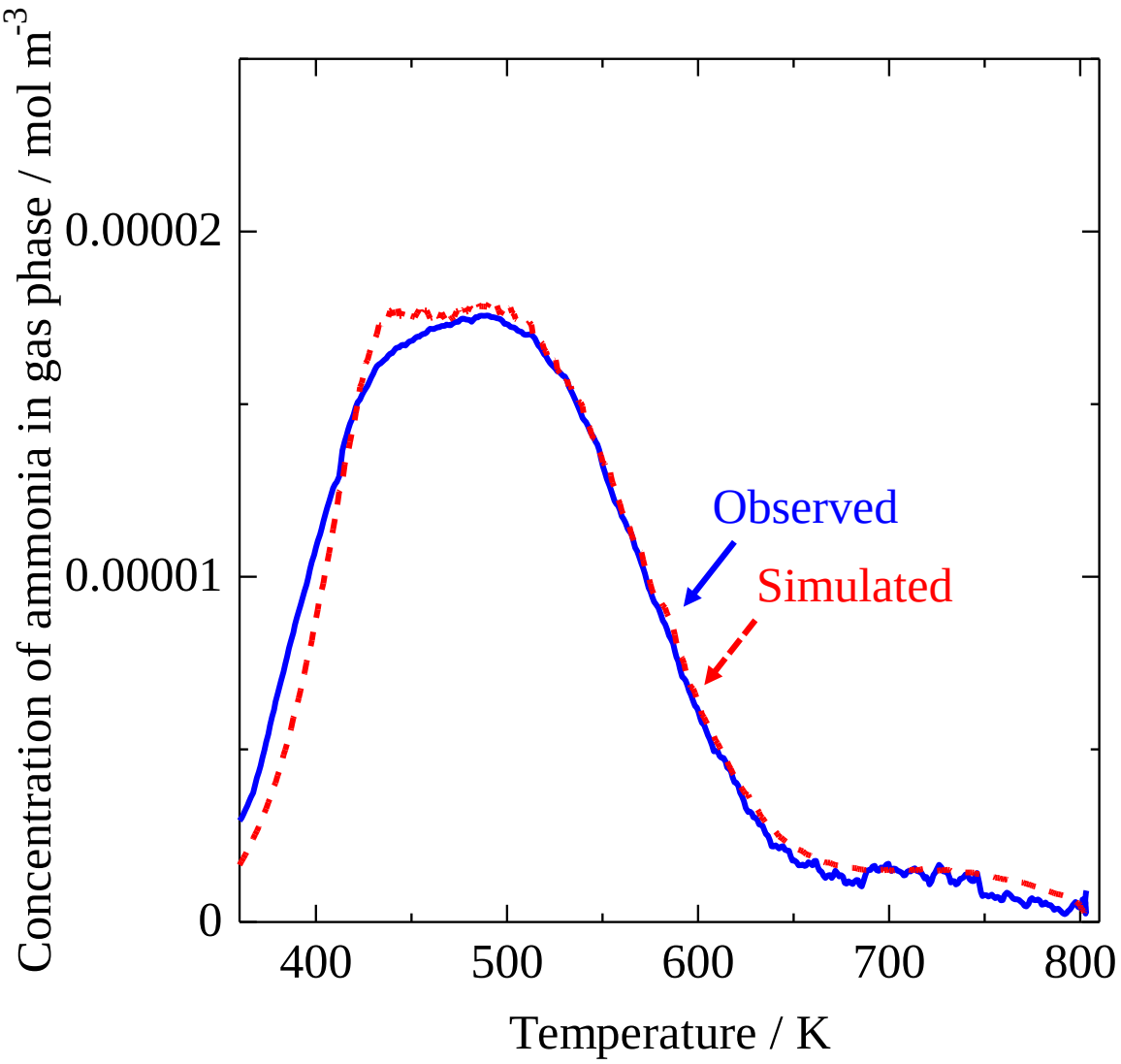
Concentration of ammonia in gas phase / mol m-3
0.00002
0.00001
0
400
500
600
700
800
Temperature / K
Observed
Simulated

Figure 8 (A)

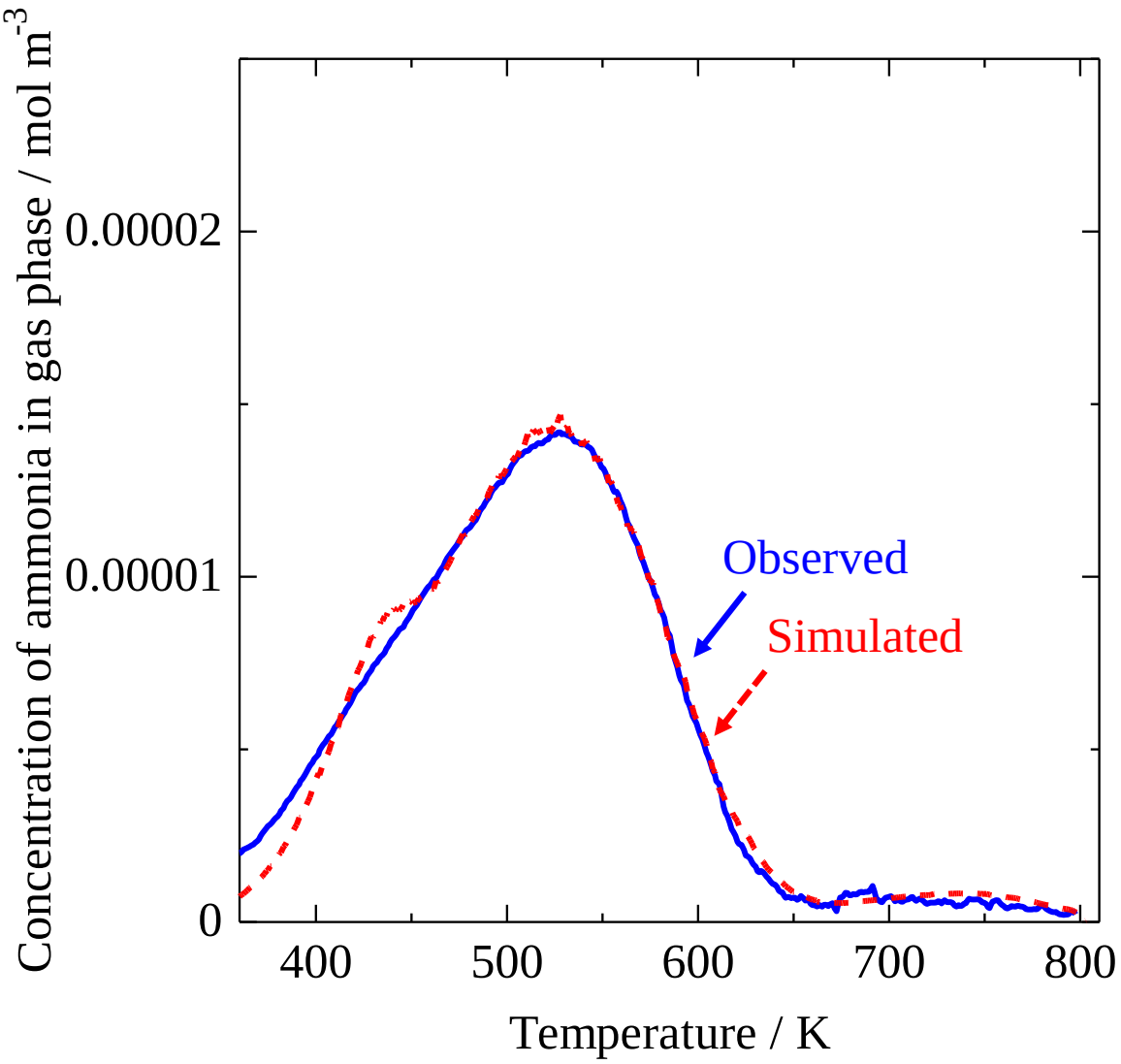
Concentration of ammonia in gas phase / mol m-3
0.00002
0.00001
0
400
500
600
700
800
Temperature / K
Observed
Simulated

Figure 8 (B)

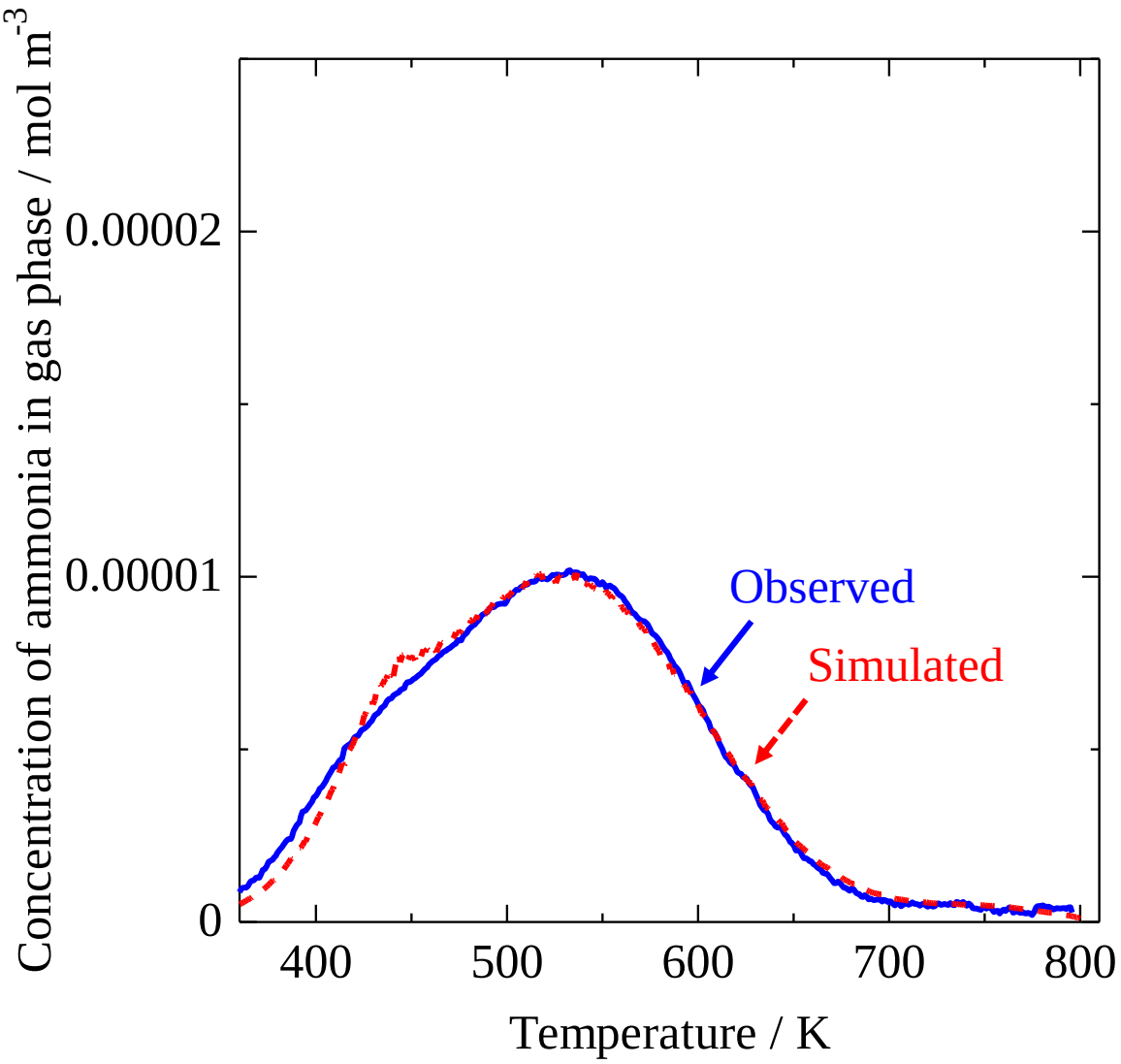
Concentration of ammonia in gas phase / mol m-3
0.00002
0.00001
0
400
500
600
700
800
Temperature / K
Observed
Simulated

Figure 8 (C)

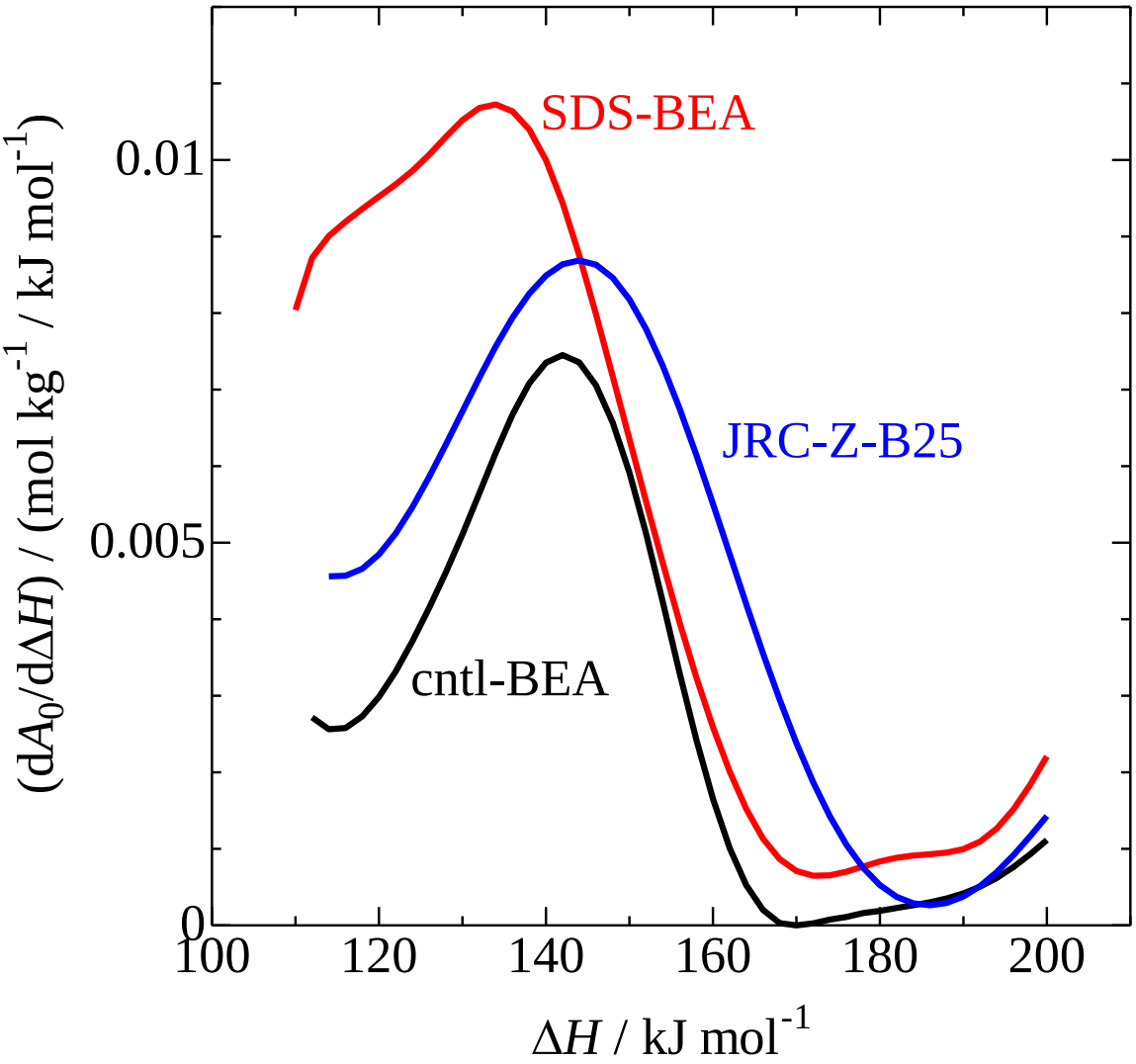
SDS-BEA
JRC-Z-B25
cntl-BEA
0.01
0.005
0
100
120
140
160
180
200
(dA0/dΔH) / (mol kg-1 / kJ mol-1)
ΔH / kJ mol-1

Figure 9